

Muon-Spin Rotation Spectra in the Mixed Phase of High- T_c Superconductors : Thermal Fluctuations and Disorder Effects

Gautam I. Menon[†]

Department of Physics,

Simon Fraser University, Burnaby

B.C. V5A 1S6, Canada

Chandan Dasgupta[‡] and T. V. Ramakrishnan[‡]

Department of Physics, Indian Institute of Science,

Bangalore – 560 012, India.

(May 12, 2018)

Abstract

We study muon-spin rotation (μ SR) spectra in the mixed phase of highly anisotropic layered superconductors, specifically $Bi_{2+x}Sr_{2-x}CaCu_2O_{8+\delta}$ (BSCCO), by modeling the fluid and solid phases of pancake vortices using liquid-state and density functional methods. The role of thermal fluctuations in causing motional narrowing of μ SR lineshapes is quantified in terms of a first-principles theory of the flux-lattice melting transition. The effects of random point pinning are investigated using a replica treatment of liquid state correlations and a replicated density functional theory. Our results indicate that motional narrowing in the pure system, although substantial, cannot account for the remarkably small linewidths obtained experimentally at relatively high fields and low temperatures. We find that satisfactory agreement with the μ SR data for BSCCO in this regime can be obtained through the *ansatz* that this “phase” is characterized by *frozen* short-range

positional correlations reflecting the structure of the liquid just above the melting transition. This proposal is consistent with recent suggestions of a “pinned liquid” or “glassy” state of pancake vortices in the presence of pinning disorder. Our results for the high-temperature liquid phase indicate that measurable linewidths may be obtained in this phase as a consequence of density inhomogeneities induced by the pinning disorder. The results presented here comprise a unified, first-principles theoretical treatment of μ SR spectra in highly anisotropic layered superconductors in terms of a controlled set of approximations.

PACS: 74.60.-w, 74.72.Hs, 76.75.+i

I. INTRODUCTION

In the mixed phase of a type-II superconductor, an externally applied magnetic field penetrates the bulk of the sample in the form of lines of magnetic flux [1]. The distribution function $n(B)$ of the local magnetic induction B in the sample is thus a non-trivial quantity, depending on the flux distribution associated with a single vortex line, as well as on the arrangement of the vortex lines in space and time. This distribution function can be obtained through muon-spin rotation (μ SR) experiments based on the following procedure: An ensemble of muons, initially polarized transverse to the magnetic induction, is implanted uniformly throughout the sample [2,3,4]. Since the local magnetic induction varies in space, the spins of the muons in different regions of the sample precess at different rates, resulting in a dephasing of the initial polarization with time. This dephasing is monitored by tracking the angular distribution of the positrons emitted as the muons decay. The measured polarization can then be related, via a Fourier transform, to $n(B)$.

The utility of the μ SR method is that it provides an accurate local probe of magnetic field variations in the bulk irrespective of whether such variations are periodic (as for a regular vortex lattice) or have more complex structure reflecting arrangements of vortex lines with varying degrees of spatial correlations. In high-temperature superconductors such as $Bi_{2+x}Sr_{2-x}CaCu_2O_{8+\delta}$ (BSCCO), μ SR experiments carried out in a field perpendicular to the superconducting layers (this is the geometry we consider throughout this paper) have provided indirect evidence for what is believed to be a melting transition [5] of the Abrikosov flux-line lattice to a flux liquid with short-ranged positional correlations. In the experiments of Lee *et al* [6,7,8] on BSCCO, where $n(B)$ is obtained as a function of the external field H and the temperature T , the location of the melting line at fields of the order of 10 mT is inferred from the abrupt changes in the μ SR linewidths and lineshapes which occur as H and/or T are varied across the transition boundary. In this low-field regime, the results obtained are in broad agreement with extensive experimental and theoretical work over the past decade aimed at detecting and understanding the nature of such a melting transition.

In contrast, the nature of the transition and of the low-temperature phase at *high* fields still remains controversial.

For a regular Abrikosov lattice at zero temperature and in the absence of disorder, the second moment of $n(B)$ can be simply related to the magnetic penetration depth λ [3]. For a wide variety of superconductors, the values of λ obtained in this way [9,10,11] agree closely with those obtained by other means [12]. However, for BSCCO, such an interpretation of the high field data yields values for the ab plane penetration depth λ_{ab} ranging between 3500 and 4500 Å [13]. These numbers are to be contrasted to typical values obtained by other means which suggest $1100 < \lambda_{ab} < 2800\text{Å}$, with values in the range $1500 < \lambda_{ab} < 2000\text{Å}$ believed to be appropriate for slightly overdoped samples [7,8,14,15,16]. This discrepancy originates in the anomalously small values of the linewidth $\sqrt{[\Delta B^2]}$ (the brackets $[\cdot \cdot \cdot]$ denote a space average) obtained in experiments performed at high fields [17]. Fits to the lineshapes at low fields, in contrast, yield results in reasonable agreement with conventionally accepted values for λ_{ab} with $\lambda_{ab} \simeq 1800\text{Å}$ obtained in the recent experiments of Lee *et al.* [6,7,8]. The magnitude of the linewidths is found to change rather sharply across a “critical” value H_{cr} (~ 100 mT) of the magnetic field which depends only weakly on the temperature (the “low” and “high” field regimes referred to earlier can be more precisely correlated to H_{cr}). As the external field is increased across H_{cr} , the μSR lineshapes are observed to become far more symmetric, concomitant with the sharp reduction in linewidths. This asymmetry can be quantified through the normalized “asymmetry parameter” $\alpha = [\Delta B^3]^{1/3}/[\Delta B^2]^{1/2}$. In the high field regime, measured values of α range from 0.5 – 0.9 ($\alpha \simeq 1.2$ in the Abrikosov flux lattice phase). These observations suggest that the nature of the flux array changes qualitatively as the applied field is increased across H_{cr} . The existence of such a critical field value across which the attributes of the flux-line system change abruptly has been confirmed in a variety of other measurements, including transport [18] and magnetization [19] experiments and neutron scattering [20]. Possible explanations for these observations include the proposal of a sharp crossover from three-dimensional to effectively two-dimensional behavior as a function of the field in the absence of disorder [21],

an entanglement transition of the flux-line lattice [22,23] as the field is increased, and the transition between a pinning-induced, weakly disordered “Bragg glass” phase [24] at low field values [25,26] to a strongly disordered “pinned liquid” or “vortex glass” [27] phase at high fields. Figs. VII–3 illustrate schematic phase diagrams. The phase diagram of a pure system according to the conventional Abrikosov theory is shown in Fig. VII. A phase diagram illustrating the Abrikosov lattice and vortex liquid phases expected for a pure system is shown in Fig. 2, and Fig. 3 shows a conjectured phase diagram in the presence of random point pinning, illustrating Bragg glass, pinned liquid (or vortex glass) and vortex liquid phases.

The explanations proposed for reduced linewidths in the high field regime of BSCCO fall into two major classes which are not completely unrelated. One class of theories suggests that reduced linewidths arise due to thermal broadening (and possibly quantum broadening – we ignore quantum effects in the bulk of this paper, but discuss them briefly in the concluding section) of density distributions in the lattice phase. It is argued that the effects of thermal fluctuations in BSCCO are enhanced above H_{cr} due to the nearly two-dimensional character of vortex fluctuations in this regime – the flux-line structure in BSCCO is more accurately thought of in terms of “pancake” vortices [28] moving on the superconducting layers and interacting via a combination of electromagnetic and Josephson couplings. Such behavior should generalize to all sufficiently anisotropic, layered compounds [29] and should be reflected to a lesser extent in more isotropic materials. Calculations representing this class of theories have so far been restricted to harmonic treatments of elastic fluctuations about the zero-temperature Abrikosov flux lattice [7,8,29,30]. In these calculations, the effects of thermal fluctuations in the lattice phase are expressed in terms of the Lindemann parameter $L = \sqrt{\langle u^2 \rangle} / a_0$, where $\langle u^2 \rangle$ is the mean square thermal fluctuation of a flux-line from its equilibrium position at melting and a_0 is the mean inter-line spacing. In the analysis of experimental data, L is treated as a phenomenological fitting parameter. One purpose of this paper is to present calculations of μ SR lineshapes and linewidths based on a detailed and microscopic theory of flux-liquid and flux-lattice phases in a highly anisotropic layered

superconductor. This theory can be used to *calculate* the Lindemann parameter as well as density distributions at freezing. Such density distributions feed into a calculation of the lineshapes measurable in μ SR experiments – results of a calculation of these lineshapes are presented here.

The second class of theories invokes the presence of underlying quenched disorder and proposes random pinning as a possible source of reduced linewidths. The quasi-two-dimensional vortex system above H_{cr} is argued to be highly susceptible to pinning. Several proposals for the nature of this low-temperature state exist in the literature. The “vortex glass” description [27] concentrates on the physics at large length scales and thus does not address issues of short-range order. There has been much recent interest in the proposal [25] that at low fields, the flux-line system is in a “Bragg glass” phase in which the δ -function Bragg peaks associated with the pure crystalline phase are replaced by algebraic singularities. Such a relatively ordered phase is expected [22,25,26] to yield to a topologically disordered phase (where dislocations proliferate) at fields larger than a critical value, this transition being driven by the increasing relevance of disorder due to the effective reduction of the dimensionality at high fields. Evidence for such a transition has been found in numerical simulations [31] of a system of flux lines in the presence of random point pinning. The Bragg glass scenario is a plausible explanation of the experimental data. However, the precise nature of the phase obtained at large fields remains unclear. Given that the physics of the problem at high fields is dominated by the fluctuations of pancake vortices weakly coupled across layers, correlations of vortices across the superconducting layers are expected to be much weaker than correlations between vortices on the same layer. Specifically in the context of μ SR experiments on BSCCO, some analytic work exists on a model which assumes that the low-temperature state in the presence of pinning disorder is characterized by a disordered stacking of ordered planes [30,32]. However, it is difficult to see how even relatively strong disorder could stabilize such an arrangement in which the misalignment of ordered layers is penalized by a macroscopic (proportional to the area of the layer for each layer) energy cost. It is reasonable to expect that some fraction of this cost is relaxed by

allowing dislocations to form on each layer. If a non-zero density of dislocations is allowed to form, the detailed microscopic arrangement of vortices must be qualitatively different from that proposed in such simplified models. In this paper we propose that a reasonable assumption for this disordered state is that it resembles a “frozen” liquid in the sense that the positional correlations in this state are essentially the same as that in a liquid just above its putative freezing transition, but the time scale for structural relaxation is much longer than that in the liquid.

In our theoretical analysis of μ SR spectra in the mixed phase of extremely anisotropic, layered, type-II superconductors in a field applied perpendicular to the superconducting layers, the flux-solid phase is described using the density functional theory [33,34,35,36] and the fluid phase using a liquid state-theory adapted by us [35,36] to study “pancake” vortices in the Lawrence-Doniach description [37] of a layered superconductor in the limit of vanishing Josephson coupling. Our approach assumes a value of λ_{ab} consistent with the values obtained from low-field μ SR and other experiments on BSCCO ($1500\text{\AA} < \lambda_{ab} < 1800\text{\AA}$) and calculates linewidths and lineshapes appropriate to these values, incorporating thermal fluctuations, disorder effects (we consider random point pinning produced by atomic-scale pinning centers such as oxygen defects [38]) as well as corrections due to the finite core size [39]. The approach outlined here should be applicable to the calculation of μ SR lineshapes in artificial superconducting multilayers [40] in which the distance between neighboring superconducting layers can be tuned so as to reduce the Josephson coupling between layers to an insignificant level. The approach of this paper is, in principle, non-perturbative in that our description of thermally broadened density distributions in the flux-solid phase is not restricted to assuming a harmonic form for the free energy cost associated with small deviations from the perfect lattice.

Our principal results for the pure system include a calculation of μ SR lineshapes and linewidths at freezing. These results can be extended below the freezing transition by *assuming* harmonic fluctuations at sufficiently low-temperatures, whose magnitude is consistent with the theoretically calculated $\langle u^2 \rangle$ at the melting transition. We find that thermal

broadening should reduce the μ SR linewidth for BSCCO at the flux-lattice melting temperature by a factor of about 4 relative to that for a perfect Abrikosov lattice. These results quantify thermal fluctuation amplitudes in the pure system and the magnitude of the corresponding corrections to the linewidths. These corrections can then be used to estimate λ_{ab} more accurately. However, the linewidths so obtained are still far in excess of those measured experimentally for $H \gg H_{cr}$ even at the “melting” transition. Further, theories based on thermal fluctuations about an ordered triangular lattice of flux lines cannot explain the anomalously small linewidths obtained at low temperatures, as pointed out by several other authors. Thus, disorder effects appear to be necessary for an explanation of the μ SR linewidths at high fields.

We also study, using a replicated liquid-state and density functional theory [41], the effects of weak pinning disorder on the μ SR linewidth in both the high-temperature liquid and the low-temperature solid. We find that such disorder should not affect μ SR lineshapes considerably in the low-temperature state *if it has strong local crystalline order*, such as might be expected in a state composed of “Larkin domains” [42] of characteristic size much larger than the average inter-vortex spacing, and in a Bragg glass phase with algebraic decay of positional correlations. The fact that pinning should affect the lineshapes only weakly in such a state is expected on intuitive grounds because only the *short-range* order of the arrangement of the vortices is probed in μ SR experiments. However, these results disagree with experimental observations in the high-field limit, indicating that the system cannot have strong short-range crystalline order in this regime. In the absence of a detailed theory of the structure of the flux-line system in this regime, we propose that *the positional correlations in this state resemble those in the liquid just above the solid-liquid “transition”*. This state, however, differs from the high-temperature liquid in that the characteristic time scale for structural relaxation is much longer than that in the liquid. The correlations probed in the μ SR experiments are then naturally understood as being representative of the positional correlations in the equilibrated liquid. This proposal is consistent with the “pinned liquid” state postulated in the phase diagram suggested in Ref. [25]. This description should also

be appropriate if the high-field, low-temperature state of the system represents a new glassy phase that is separated from the high-temperature liquid by a line of true phase transitions. This is because the positional correlations in a structural glass are generally quite similar to those in the liquid near the glass transition. We present calculations of the second and third moments (the third moment is calculated using a specific decoupling approximation for correlations) of the field distribution in such a low-temperature disordered state and find that the results (summarized in Table I) are in good agreement with the experimental data on BSCCO.

Several time scales are relevant to the analysis of transverse μ SR spectra in the mixed phase. A muon injected into the sample at time $t = 0$ thermalizes due to interactions with the bulk material on timescales of order 10^{-10} s [3]. This time scale is much shorter than the muon lifetime and typical precession times ($\sim 10^{-6} - 10^{-7}$ s). After thermalization, the muon diffuses in the sample. If the diffusivity of the muons is small, the typical distance traveled by a muon during its lifetime is much smaller than both the mean inter-vortex spacing and the penetration depth. In this limit, which is the one we consider, the polarization after time t is completely determined by the initial polarization and the distribution of local fields. (A complication that may be present in real experiments is that the muons may be preferentially absorbed at certain sites. We do not consider this possibility in the present work and assume that the muons are uniformly distributed.) Other time scales that enter the problem are the relaxation times of density fluctuations in the solid and liquid phases, which determine the time scales over which the field felt by a stationary muon varies. For the pure system, consistent with other work and with results obtained on $\text{YBa}_2\text{Cu}_3\text{O}_{7-\delta}$ (YBCO) and other high- T_c superconductors, we assume that the relaxation time in the low-temperature (lattice) phase is very short relative to the inverse precession rate of the muons. (Experimentally, these time scales are found to be of order 10^{-10} s [43] close to the flux-lattice melting transition.) In the fluid phase, the μ SR linewidth would be expected to be vanishingly small due to motional narrowing if the vortex lines are highly mobile. However, if the vortex lines have very low mobility, such as might be expected in

strongly pinned, entangled or glassy states, the second moment of $n(B)$ can be related to the static structure factor of the liquid. We argue that the low mobility situation is realized at low temperatures in the high-field state of the pancake vortex system in the presence of random point pinning. At high temperatures and deep into the fluid regime, we argue that the vortex lines are highly mobile, so that the structural relaxation times of the vortex system are much shorter than the inverse precession rate of the muons. Even in this regime, there is a non-vanishing contribution to linewidths that comes from a space-averaged correlation function of pinning-induced density inhomogeneities in the liquid. We present a calculation of this contribution to the second moment of the field distribution function. Our results are representative of the linewidths obtained experimentally deep into the liquid phase.

The outline of this paper is as follows. In section II, we briefly discuss the calculation of the field distribution and its moments in a perfect Abrikosov lattice. In section III, we introduce our model of “pancake” vortices confined to the superconducting planes, and briefly describe the liquid-state and density functional methods used in our study. We also discuss the replica method we use to study the disordered liquid and its freezing transition in the presence of random point pinning. In section IV, we calculate the magnetic field distribution and its moments for a thermally broadened Abrikosov lattice. We use the density functional description of the crystalline solid phase of the vortex system [35,36] in our analysis. In section V, we calculate these moments in a “frozen” liquid state of the vortex system. We provide calculations of the second and third moments to support our proposal that values of $[\Delta B^2]$ consistent with λ_{ab} values of about 1800\AA can be obtained if it is assumed that the low-temperature state of the vortex system at high fields is a glassy one characterized by short-ranged, liquid-like correlations and long relaxation times. The effects of weak disorder on the second moment of the field distribution in the high-temperature liquid state are discussed in section VI, where we point out that non-vanishing linewidths can be obtained in this state by considering the contribution from the static inhomogeneities induced in the liquid by the quenched disorder. Section VII contains a summary of the main results obtained in this paper and a few concluding remarks.

II. μ SR SPECTRUM FOR AN IDEAL ABRIKOSOV LATTICE

The time evolution of the transverse polarization ($P^+(\mathbf{r}, t) = P_x(\mathbf{r}, t) + iP_y(\mathbf{r}, t)$) of a muon in a locally inhomogeneous magnetic field $\mathbf{B}(\mathbf{r})$, assumed to lie in the \hat{z} direction (i.e. $\mathbf{B}(\mathbf{r}) = \hat{z}B(\mathbf{r})$), is given by the Bloch-Torrey equation [44]

$$\frac{\partial P^+(\mathbf{r}, t)}{\partial t} = -i\gamma_\mu B(\mathbf{r})P^+(\mathbf{r}, t) + D\nabla^2 P^+(\mathbf{r}, t), \quad (2.1)$$

where D is the muon diffusivity, $P_x(\mathbf{r}, t), P_y(\mathbf{r}, t)$ are the two components of the polarization transverse to the field and γ_μ is the muon gyromagnetic ratio ($= 8.516 \times 10^8 \text{ rad T}^{-1} \text{ s}^{-1}$). Eq.(2.1) is to be solved subject to the initial condition $P^+(\mathbf{r}, t = 0) = P_i^+(\mathbf{r})$. If the initial distribution of muons is uniform then $P^+(\mathbf{r}, t = 0) = P^0$ and if, in addition, the muon does not diffuse, the solution of Eq.(2.1) is

$$P^+(\mathbf{r}, t) = P^0 \exp[-i\gamma_\mu B(\mathbf{r})t]. \quad (2.2)$$

The space averaged distribution of the local magnetic induction is defined as

$$n(B) = [\delta(B - B(\mathbf{r}))], \quad (2.3)$$

where $[A(\mathbf{r})]$ refers to the space average $(1/V) \int_V d\mathbf{r} A(\mathbf{r})$, V being the volume of the sample. It then follows that

$$P^{(+)}(t) = \frac{P^{(0)}}{\gamma_\mu} \int_{-\infty}^{+\infty} n\left(\frac{\omega}{\gamma_\mu}\right) \exp(-i\omega t) d\omega, \quad (2.4)$$

where $P^{(+)}(t)$ is the spatial average of $P^{(+)}(\mathbf{r}, t)$ and $\gamma_\mu B = \omega$. The measured $P^{(+)}(t)$ can then be used to obtain, through an inverse Fourier transformation, the distribution of internal fields in the sample.

The local magnetic field at a point \mathbf{r} due to an array of straight vortex lines in the \hat{z} direction is given by

$$B(\mathbf{r}) = \int d\mathbf{r}' b(|\mathbf{r} - \mathbf{r}'|) \rho(\mathbf{r}'), \quad (2.5)$$

where $b(\mathbf{r}-\mathbf{r}')$ denotes the field at point \mathbf{r} due to a single vortex line at \mathbf{r}' and $\rho(\mathbf{r})$ is the flux line density at point \mathbf{r} (\mathbf{r} is a two-dimensional vector perpendicular to the z -axis). Using the Fourier decomposition $\rho(\mathbf{r}') = (1/A) \sum_{\mathbf{k}} \rho_{\mathbf{k}} \exp(i\mathbf{k} \cdot \mathbf{r}')$, and $b(\mathbf{r}) = (1/A) \sum_{\mathbf{k}} b_{\mathbf{k}} \exp(i\mathbf{k} \cdot \mathbf{r})$ (A is the cross sectional area of the sample) we get

$$B(\mathbf{r}) = (1/A) \sum_{\mathbf{k}} b_{\mathbf{k}} \rho_{\mathbf{k}} \exp(i\mathbf{k} \cdot \mathbf{r}). \quad (2.6)$$

In an Abrikosov lattice, only terms involving reciprocal lattice vectors ($\mathbf{k} = \mathbf{G}$) survive in Eq.(2.6). For a perfect lattice with δ -function densities, $\rho_{\mathbf{G}} = N$ for all \mathbf{G} (N is the number of flux lines) and the sum may be written as

$$B(\mathbf{r}) = \frac{B_0}{\Phi_0} \sum_{\mathbf{G}} b_{\mathbf{G}} \exp(i\mathbf{G} \cdot \mathbf{r}), \quad (2.7)$$

where $N\Phi_0 = B_0A$ and B_0 is the magnetic induction within the sample, averaged over distances of order the penetration depth. Φ_0 is the quantum unit of flux carried by each line and equals 2.07×10^{-15} T m². In the London model,

$$b_{\mathbf{G}} = \frac{\Phi_0}{1 + \lambda^2 G^2}, \quad (2.8)$$

with $G^2 = G_x^2 + G_y^2$, which leads to a magnetic induction that diverges logarithmically at the core of a vortex. This unphysical divergence can be eliminated by introducing a core ‘‘form factor’’ $f(G)$ which represents the behavior near the core more accurately. This then gives

$$b_{\mathbf{G}} = \frac{\Phi_0 f(G)}{1 + \lambda^2 G^2}, \quad (2.9)$$

Analytic expressions for $f(G)$ can be obtained from solutions of the full Ginzburg-Landau equations at low inductions. A variational solution to these equations by Clem [45] yields the result $f(G) = gK_1(g)$, where $g = \sqrt{2}\xi(G^2 + \lambda^{-2})^{1/2}$. Here, ξ is the coherence length of the superconductor and $K_1(x)$ is a modified Bessel function. A less accurate but more commonly used representation of this core form factor replaces $gK_1(g)$ by the Gaussian form $\exp(-\xi^2 G^2/2)$. Recently, Yaouanc *et al* [39] have argued that it is essential to retain the full

form of the core form factor for a satisfactory treatment. Using results originally derived by Hao *et al* [46], they obtain

$$B(\mathbf{r}) = B_0 \sum_{\mathbf{G}} \frac{w(G)K_1(w(G))(1-b^4)}{(1+\lambda^2 G^2)} \exp(i\mathbf{G} \cdot \mathbf{r}), \quad (2.10)$$

where $w^2(G) = 2(\xi^2 G^2)(1+b^4)[1-2b(1-b)^2]$, $b = B_0/B_{c2}$, and we have specialized their expressions to the case in which there are no in-plane anisotropies. For the triangular Abrikosov lattice, the sum in Eq.(2.10) is to be carried out over the reciprocal lattice generated by the vectors $\mathbf{G}_1 = (4\pi/\sqrt{3}a_0)\hat{y}$ and $\mathbf{G}_2 = (2\pi/a_0)[\hat{x} + \hat{y}/\sqrt{3}]$. Here the inter-vortex spacing a_0 is given by $a_0^2 = 2\Phi_0/\sqrt{3}B_0$. For the calculations reported in this paper, we use the full form factor proposed by Yaouanc *et al.* in our description of lineshapes and linewidths in both solid and fluid phases. Also, since we work at inductions much less than B_{c2} , we set $b^4 \simeq 0$ and $[1-2b(1-b)^2] \simeq 1$.

The moments of the field distribution function $n(B)$ can be obtained from Eq.(2.10). The second moment of the distribution function $[\Delta B^2] \equiv \int_{-\infty}^{+\infty} n(B)(B-B_0)^2 dB$ is obtained as

$$[\Delta B^2] = B_0^2 \sum_{\mathbf{G} \neq 0} \frac{w^2(G)K_1^2(w(G))}{(1+\lambda^2 G^2)^2} \simeq B_0^2 \sum_{\mathbf{G} \neq 0} \frac{w^2(G)K_1^2(w(G))}{\lambda^4 G^4}, \quad (2.11)$$

where

$$G^2 = \frac{16\pi^2}{3a_0^2} [m^2 + mn + n^2], \quad (2.12)$$

m, n are integers and we have used $\lambda/a_0 \gg 1$ in obtaining the final answer in Eq.(2.11). The third moment, defined by $[\Delta B^3] \equiv \int_{-\infty}^{+\infty} n(B)(B-B_0)^3 dB$ is obtained as

$$[\Delta B^3] = B_0^3 \sum_{\substack{\mathbf{G}_1, \mathbf{G}_2, \mathbf{G}_3 \neq 0 \\ \mathbf{G}_1 + \mathbf{G}_2 + \mathbf{G}_3 = 0}} \frac{\sigma(G_1)\sigma(G_2)\sigma(G_3)}{(1+\lambda^2 G_1^2)(1+\lambda^2 G_2^2)(1+\lambda^2 G_3^2)}, \quad (2.13)$$

where the $\sigma(G_i)$, $i = 1, 2, 3$, represent the cutoff corrections and are given by

$$\sigma(G_i) = w(G_i)K_1(w(G_i)). \quad (2.14)$$

III. MODEL AND METHODS OF CALCULATION

In extremely anisotropic, layered superconductors in their type-II regime in an external field applied perpendicular to the layer plane, the statistical mechanics of the interacting flux-line system reduces to the problem of interacting planar vortices. These “pancake” vortices are formed at the intersections of the flux lines with the planes on which the superconducting order parameter $\Psi(r)$ attains its maximum value. In the limit of infinite anisotropy (a reasonably accurate starting point for BSCCO in which the anisotropy factor γ has been estimated to be higher than 100), the pancake vortices interact via a pair-wise potential that can be calculated within the framework of a London model [47]. This limit corresponds to assuming that the direct Josephson coupling between two adjacent superconducting layers is vanishingly small. However, vortices on different layers continue to be coupled through their electromagnetic interaction. Recent studies [8,16] have shown that in BSCCO, the electromagnetic interaction between vortices dominates over the interaction generated by the Josephson coupling if the temperature is lower than about $0.8T_c(0)$. As the low-temperature behavior will be our primary concern in this paper, our assumption of infinite anisotropy can be expected to be quite reasonable for BSCCO.

As we have argued earlier [35,36], the statistical mechanics of the flux-line system in its fluid phase is most easily approached in this limit by considering the system of pancake vortices to be a classical, anisotropic liquid. The equilibrium density correlation functions of this classical liquid may be calculated by generalizing methods of liquid-state theory, and the freezing transition of this liquid may be studied using well known methods of classical density functional theory with the calculated liquid-state correlation functions as input. Such an approach makes it possible to characterize thermally broadened density distributions in the equilibrium solid at the freezing transition without using any *ad hoc* assumption.

In this section, we first define the effective “Hamiltonian” of the vortex system in the limit of infinite anisotropy, and then provide brief introductions to the liquid-state and density functional methods used in our analysis. Finally, we discuss the techniques we use to study

the effects of disorder on liquid state correlations and the extension of density functional methods to deal with the problem of freezing in the presence of random pinning.

A. Interaction between pancake vortices in the limit of infinite anisotropy

If the coherence length of a layered superconductor in the direction perpendicular to the layers is of the order of the inter-layer spacing d , the appropriate generalization of the Ginzburg-Landau functional is a free-energy functional suggested by Lawrence and Doniach [37]. In the limit of infinite anisotropy (i.e. vanishing Josephson coupling between the superconducting layers), the Lawrence-Doniach functional in the “phase-only” (London) approximation reduces to a particularly simple form from which the interaction energy of a collection of pancake vortices can be readily derived [47,48]. The energy turns out to be a sum of pairwise interactions (this simplification occurs only in the limit of infinite anisotropy – the effective “Hamiltonian” of a system of pancake vortices can not be broken up into a sum of pairwise terms if the Josephson coupling is finite). In Fourier space, the inter-vortex interaction is given by

$$\beta V(\mathbf{k}) = \frac{\Gamma \lambda^2 [k_{\perp}^2 + (4/d^2) \sin^2(k_z d/2)]}{k_{\perp}^2 [1 + \lambda^2 k_{\perp}^2 + 4(\lambda^2/d^2) \sin^2(k_z d/2)]}, \quad (3.1)$$

with $\Gamma = \beta d \Phi_0^2 / 4\pi \lambda^2$ (λ is the in-plane penetration depth – we have removed the subscript ab for ease of notation) and $\beta = 1/k_B T$. In Eq.(3.1), k_{\perp} and k_z refer, as before, to directions in the plane of the layers and normal to them. Two vortices lying on the same layer repel each other with a potential that is a logarithmic function of their separation, whereas two vortices on different layers *attract* each other with a potential that is weaker than the intralayer potential by the factor d/λ . The interlayer potential is logarithmic in the in-plane separation and falls off exponentially in the z -direction as $e^{-nd/\lambda}$ where n is the layer separation.

The Fourier transforms of the radial and z -axis components of the magnetic field due to a single pancake vortex at the origin are given by

$$\mathbf{b}_{\perp} = -\frac{d\Phi_0 k_z \mathbf{k}_{\perp}}{k_{\perp}^2 (1 + \lambda^2 k_{\perp}^2 + \lambda^2 k_z^2)}, \quad (3.2)$$

and

$$b_z = \frac{d\Phi_0}{(1 + \lambda^2 k_\perp^2 + \lambda^2 k_z^2)}, \quad (3.3)$$

The calculation of local field distributions and their moments in this case proceeds in much the same way as outlined in the previous section. In this description, however, there is also a radial component associated with the total magnetic induction. (This component vanishes in the case of perfectly aligned straight vortex lines). In addition, the z -axis component of the magnetic induction is a weak function of z , even for a straight line of pancake vortices. If the inter-layer spacing is small, however, in comparison to the length scale over which the field varies (i.e. $d \ll \lambda$), this variation can be neglected.

B. Liquid state correlations and density functional theory for the pure vortex system

A basic quantity that appears in a statistical description of the equilibrium properties of a simple isotropic liquid is the pair distribution function $g(|\mathbf{r} - \mathbf{r}'|)$, defined by $\langle \sum_{i=1}^N \sum_{j \neq i}^N \delta(\mathbf{r} - \mathbf{r}_i) \delta(\mathbf{r}' - \mathbf{r}_j) / \rho_\ell^2 \rangle$. Here, \mathbf{r}_i denotes the location of the i th particle in the liquid and ρ_ℓ is the average density. The pair correlation function $h(r)$ defined by $h(r) = g(r) - 1$, and the static structure factor defined by $S(k) = 1 + \rho_\ell \int d\mathbf{r} h(r) \exp(i\mathbf{k} \cdot \mathbf{r})$ are closely related to $g(r)$. The pair correlation function can be decomposed as

$$h(r) = C(r) + \rho_\ell \int d\mathbf{r}' C(|\mathbf{r} - \mathbf{r}'|) h(\mathbf{r}'), \quad (3.4)$$

which is the Ornstein-Zernike relation [49]. The Fourier transform of the direct pair correlation function $C(r)$ is related to the structure factor through $S(k) = 1/(1 - \rho_\ell C(k))$.

These definitions can be readily generalized [35,36] to describe the equilibrium correlations in a layered liquid of pancake vortices. Since this system is highly anisotropic, the two-point correlation functions in position space have two arguments: the in-plane separation ρ and the separation nd in the z -direction (n is an integer). The Fourier transforms of these functions depend separately on k_z and k_\perp . As discussed in detail in Refs. [35] and

[36], standard methods of liquid state theory, such as the Hypernetted Chain approximation (HNC) [49] and the Rogers-Young closure scheme [50], can be generalized to calculate these correlation functions of the layered vortex liquid. These correlation functions are then used as input to a density functional theory of freezing from which the freezing temperature and the time-averaged density distributions in the solid phase at the freezing transition are obtained.

In the density functional theory, the free energy of an inhomogeneous configuration of the time-averaged density field is expressed in terms of fluid-phase correlation functions. Freezing into a crystalline structure occurs when the free energy of the state with the appropriate periodic density modulation equals the free energy of the uniform liquid. In the density functional theory of Ramakrishnan and Yussouff [33], the grand-canonical free energy cost (with respect to the uniform liquid) of producing a time-averaged density inhomogeneity is expressed as a functional of the density $\rho(\mathbf{r})$. The simplest such functional for an isotropic system is

$$\frac{\Delta\Omega}{k_B T} = \int d\mathbf{r} \left[\rho(\mathbf{r}) \ln \frac{\rho(\mathbf{r})}{\rho_\ell} - \delta\rho(\mathbf{r}) \right] - \frac{1}{2} \int d\mathbf{r} \int d\mathbf{r}' C(|\mathbf{r} - \mathbf{r}'|) \delta\rho(\mathbf{r}) \delta\rho(\mathbf{r}') + \dots, \quad (3.5)$$

where $\rho(\mathbf{r})$ is the density at point \mathbf{r} , $\delta\rho(\mathbf{r}) \equiv \rho(\mathbf{r}) - \rho_\ell$, T is the temperature, ρ_ℓ is the liquid density and the ellipsis denotes higher order terms which are conventionally set to zero.

In mean-field theory, density configurations which represent the equilibrium phase minimize Eq.(3.5), i.e. satisfy $\delta\Delta\Omega/\delta\rho(\mathbf{r}) = 0$. This condition gives

$$\ln \left[\frac{\rho(\mathbf{r})}{\rho_\ell} \right] = \int d\mathbf{r}' C(|\mathbf{r} - \mathbf{r}'|) [\rho(\mathbf{r}') - \rho_\ell]. \quad (3.6)$$

A periodic (crystalline) density configuration is a solution of the mean-field equations if the following self-consistency condition is satisfied:

$$1 + \eta + \sum_{\mathbf{G} \neq 0} \rho_{\mathbf{G}} \exp(i\mathbf{G} \cdot \mathbf{r}) = \exp \left[\tilde{C}_0 \eta + \sum_{\mathbf{G} \neq 0} \tilde{C}_{\mathbf{G}} \rho_{\mathbf{G}} \exp(i\mathbf{G} \cdot \mathbf{r}) \right], \quad (3.7)$$

where the \mathbf{G} s are the reciprocal lattice vectors of the structure to which the liquid freezes, $\rho_{\mathbf{G}}$ s are the Fourier components of the density field with wave vector \mathbf{G} and we have defined

$\tilde{C} \equiv \rho_\ell C$. The quantity η is the fractional volume change on freezing from the liquid. Note that the uniform liquid, for which $\rho_{\mathbf{G}} = 0$ for all $\mathbf{G} \neq 0$ and $\eta = 0$, is always a local minimum of the free energy. However, because of the non-linearity of the self-consistency condition, periodic density-wave solutions which could be absolute minima of the free energy of Eq.(3.5) may appear as the correlations in the liquid increase. The $\rho_{\mathbf{G}}$ s which minimize the density functional represent the (mean-field) density distribution in the crystalline solid. Since the density distribution near a lattice point is not restricted to be Gaussian in a fully self-consistent theory, the thermal broadening of the peaks of the density distribution includes at least some of the anharmonic effects that are expected to be present near the melting transition. Our treatment, therefore, goes beyond the harmonic approximation made in several existing studies [7,8,29,30] of μ SR spectrum in the mixed phase.

The density functional formalism outlined above can be generalized in a straightforward manner [35,36] to a layered system of pancake vortices. The reciprocal lattice vectors that characterize the Abrikosov lattice are $(\mathbf{G}_\perp, G_z = 0)$ where the \mathbf{G}_\perp s are *two dimensional* reciprocal lattice vectors defining a triangular lattice.

C. Replica liquid state theory and density functional theory in the presence of pinning disorder

In earlier work [41], two of us developed a replica theory of the correlations of a vortex liquid in the presence of random point pinning and derived a replicated free-energy functional analogous to the Ramakrishnan-Yussouff functional to describe the freezing of this disordered liquid. We briefly summarize our methods here. Our analysis is based on the replica method [51] applied to a system of classical particles interacting via the Hamiltonian

$$H = H_{kinetic} + \frac{1}{2} \sum_{i \neq j} V(|\mathbf{r}_i - \mathbf{r}_j|) + \sum V_d(\mathbf{r}_i), \quad (3.8)$$

where $V(r)$ is a two-body interaction potential between the particles and $V_d(\mathbf{r})$ is a quenched, random, one-body potential. We assume that $V_d(\mathbf{r}_i)$ is drawn from a Gaussian distribution

of zero mean and short ranged correlations: $[V_d(\mathbf{r})V_d(\mathbf{r}')] = K(|\mathbf{r} - \mathbf{r}'|)$, with $[\dots]$ denoting an average over the disorder. Using $[\ln Z] = \lim_{n \rightarrow 0} [(Z^n - 1)/n]$, one obtains, prior to taking the $n \rightarrow 0$ limit, a replicated and disorder averaged partition function of the form

$$Z^R = \frac{1}{(N!)^n} \int \prod d\mathbf{r}_i^\alpha \exp\left(-\frac{1}{2k_B T} \sum_{\alpha=1}^n \sum_{\beta=1}^n \sum_{i=1}^N \sum_{j=1}^N V^{\alpha\beta}(|\mathbf{r}_i^\alpha - \mathbf{r}_j^\beta|)\right). \quad (3.9)$$

Here α, β are replica indices and $V^{\alpha\beta}(|\mathbf{r}_i^\alpha - \mathbf{r}_j^\beta|) = V(|\mathbf{r}_i^\alpha - \mathbf{r}_j^\beta|)\delta_{\alpha\beta} - \beta K(|\mathbf{r}_i^\alpha - \mathbf{r}_j^\beta|)$.

Our approach to the problem defined by Eq.(3.9) begins by recognizing that it resembles the partition function of a system of n ‘‘species’’ of particles, each labeled by an appropriate replica index. These particles interact via a two-body interaction which depends both on particle coordinates $(\mathbf{r}_i, \mathbf{r}_j)$ and replica indices (α, β) . This system of n species of particles can be treated in liquid state theory by considering it to be a n -component mixture and taking the $n \rightarrow 0$ limit in the Ornstein-Zernike equations governing the properties of the mixture. In the $n \rightarrow 0$ limit, assuming replica symmetry, we get the equations

$$h^{(1)}(k) = \frac{C^{(1)}(k) - \rho_\ell [C^{(1)}(k) - C^{(2)}(k)]^2}{[1 - \rho_\ell C^{(1)}(k) + \rho_\ell C^{(2)}(k)]^2}, \quad (3.10)$$

and

$$h^{(2)}(k) = \frac{C^{(2)}(k)}{[1 - \rho_\ell C^{(1)}(k) + \rho_\ell C^{(2)}(k)]^2}. \quad (3.11)$$

These equations are written in terms of the pair correlation functions $h^{\alpha\beta}$ and the direct correlation functions $C^{\alpha\beta}$ of the replicated system. The assumption of replica symmetry implies that $C^{\alpha\beta} = C^{(1)}\delta_{\alpha\beta} + C^{(2)}(1 - \delta_{\alpha\beta})$ and $h^{\alpha\beta} = h^{(1)}\delta_{\alpha\beta} + h^{(2)}(1 - \delta_{\alpha\beta})$. The physical interpretation of these correlation functions is as follows. The function $h^{(1)}$ describes the disorder-averaged equal-time (equilibrium) correlation of fluctuations of the local density, and $h^{(2)}$ represents the disorder-averaged correlation of disorder-induced deviations of the time-averaged local density from its average value ρ_ℓ .

In Ref. [41], we calculated the functions $h^{(1)}(\rho, nd)$ and $h^{(2)}(\rho, nd)$ for the layered vortex system using the HNC closure approximation. To estimate the inter-replica interaction $\beta K(\rho, nd)$, we assumed that the principal source of disorder is atomic scale pinning centers such as oxygen defects [38] which act to reduce T_c locally. This yields

$$\beta K(\rho, nd) \simeq \Gamma' \exp(-\rho^2/\xi^2) \delta_{n,0}. \quad (3.12)$$

Here $\xi \simeq 15\text{\AA}$ is the coherence length in the ab -plane, and $\Gamma' \approx 10^{-5}\Gamma^2$ for point pinning of strength $dr_0^2 H_c^2/8\pi$, where r_0 is an atomic scale length parameter and we have assumed defect densities of the order of $10^{20}/\text{cm}^3$. In Figs. 4 and 5, we show typical examples of the calculated correlation functions $g^{(1)}$ and $g^{(2)}$ obtained using this theory at two different values of T at fixed induction B_0 .

The calculated correlation functions $C^{(1)}(r)$ and $C^{(2)}(r)$ can then be used as input into an appropriately generalized version [34] of the density functional theory for a mixture of n species of particles. This leads to the following density functional in the $n \rightarrow 0$ limit:

$$\begin{aligned} \frac{\Delta\Omega}{k_B T} = & \int d\mathbf{r} \left[\rho(\mathbf{r}) \ln \frac{\rho(\mathbf{r})}{\rho_\ell} - \delta\rho(\mathbf{r}) \right] \\ & - \frac{1}{2} \int d\mathbf{r} \int d\mathbf{r}' [C^{(1)}(|\mathbf{r} - \mathbf{r}'|) - C^{(2)}(\mathbf{r} - \mathbf{r}')][\rho(\mathbf{r}) - \rho_\ell][\rho(\mathbf{r}') - \rho_\ell] \dots \end{aligned} \quad (3.13)$$

Here we have assumed that the density field is the same in all the replicas ($\rho^\alpha(\mathbf{r}) = \rho(\mathbf{r})$ for all α).

Generalization of this free energy to a layered system of pancake vortices is straightforward. In Ref. [41], we *assumed* that if the pinning disorder is weak, then the “solid” phase of the vortex system is described by a global minimum of this free energy characterized by non-zero values of the crystalline order parameters $\rho_{\mathbf{G}}$. Since we are interested in a mean-field description of a first-order transition (the flux-lattice melting transition is experimentally found to be first order if the pinning disorder is weak), this assumption is justified as long as the low-temperature state exhibits strong local crystalline order (specifically, as long as the translational correlation length in the low-temperature phase is much longer than the range of positional correlations in the liquid just above the freezing transition). Results of a full calculation of the phase-boundary obtained through this method were presented in Ref. [41]. Our principal result was that the liquid-solid phase boundary in the $(B - T)$ plane in the absence of disorder is only mildly affected by the presence of weak disorder, the suppression of this phase boundary to lower temperatures being larger at higher fields. These

predictions have been confirmed in recent experimental studies [53] of this phase boundary in electron-irradiated samples of BSCCO. In the present work, we use the results obtained in Ref. [41] for the density distribution in the “nearly crystalline” phase to analyze the effects of weak pinning disorder on μ SR lineshapes in the low-temperature, low-field state of the vortex system.

IV. μ SR SPECTRUM IN THE CRYSTALLINE PHASE OF BSCCO

In this section, we first consider the crystalline (Abrikosov lattice) phase of the vortex system in the absence of pinning disorder. If the typical time scales for phonon-like density fluctuations in this state are much shorter than the characteristic time scale of precession of the muon spin ($\sim (\gamma_\mu B)^{-1}$), the muons see a broadened (equilibrium) density distribution of flux lines. The time-averaged local magnetic field $B(\mathbf{r})$ is then obtained through the convolution relation

$$B(\mathbf{r}) = \int d\mathbf{r}' b(|\mathbf{r} - \mathbf{r}'|) \bar{\rho}(\mathbf{r}'), \quad (4.1)$$

which differs from Eq.(2.5) in that $\bar{\rho}(\mathbf{r})$ now represents the *time-averaged* density distribution. The Fourier components of the periodic time-averaged density field are given by $N\rho_{\mathbf{G}}$ where

$$\rho_{\mathbf{G}} = \int^{\mathcal{V}} d\mathbf{r} \bar{\rho}(\mathbf{r}) \exp(-i\mathbf{G} \cdot \mathbf{r}). \quad (4.2)$$

Here \mathcal{V} denotes the area of the unit cell. In thermal equilibrium, this time average is equal to a thermal average.

We calculate $\rho_{\mathbf{G}}$ by solving, in a one-order-parameter approximation [52], the self-consistent equations for the Fourier components of the periodic density field at freezing. The input direct correlation function, $C(k_\perp, k_z)$, is taken from a solution of the liquid-state equations with a Rogers-Young closure scheme [36,50]. We use parameters appropriate to BSCCO i.e. $\lambda(T = 0) = 1500 - 1800\text{\AA}$ and $d = 15\text{\AA}$ and assume a two-fluid temperature dependence of λ with $T_c(0) = 85$ K. As mentioned earlier, the relevant input correlation

function for the freezing of the vortex liquid into an Abrikosov lattice is $C(\mathbf{G}_\perp, G_z = 0)$. In Fig. 6, we plot the Fourier components $\rho_{\mathbf{G}}$ of the periodic density field (triangles) at the freezing temperature as functions of G . Note the fast decay of $\rho_{\mathbf{G}}$ at large G and the nearly Gaussian envelope of the decay. In Fig. 7, we display the magnetic field distribution for the thermally broadened Abrikosov lattice at freezing for values of the magnetic induction of (a) $B_0 = 0.3$ T and (b) $B_0 = 0.05$ T, incorporating corrections due to the finite core size (see Eq.(2.10)). The field distributions obtained in this theory are notably narrower and more symmetric than the corresponding distributions calculated for an almost perfect Abrikosov lattice shown in the same figure for comparison. This feature is seen in experiments on BSCCO [6,7,13].

Although the density functional description is in principle applicable even deep within the solid phase, it is unclear how to parametrize the appropriate input correlation functions in this case. While it is well-known that the existence of the liquid-solid transition cannot be inferred from usual liquid state methods such as the ones used by us (the correlations show no singular behaviour), using these correlation functions in a density functional description of the solid much below its crystallization temperature is questionable. The issue of how to describe the solid at temperatures far from freezing is relevant in determining the temperature dependence of the crystalline order parameters $\rho_{\mathbf{G}}$, which in turn determines the temperature dependence of the second moment of the field distribution function.

In this calculation, we extract the temperature dependence of the $\rho_{\mathbf{G}}$'s by assuming that the square of the width of the equilibrium density distribution at a lattice site is proportional to the temperature T at all temperatures lower than the melting temperature. The constant of proportionality is obtained by demanding that the solid at its melting temperature has the same Lindemann parameter as that obtained from our self-consistent density functional calculation at freezing. A linear temperature dependence of the mean square displacement also occurs in a harmonic treatment (with temperature-independent elastic constants) of the fluctuations of a vortex line about its equilibrium position at a lattice site. However, our treatment differs from a harmonic one in that the value of the mean square displacement

at the melting temperature is obtained from our density functional calculation which, as argued above, is non-perturbative and includes possible anharmonic effects.

The thermal broadening of the density distribution in the crystalline phase is calculated in the following way. Our density functional calculations [35,36] show that at fields larger than about 50 mT, the Lindemann parameter $\sqrt{\langle u^2 \rangle}/a_0$ at the freezing temperature is nearly constant at a value $\simeq 0.2$. Assuming $\langle u^2(T) \rangle/a_0^2 = \chi T$, and using the value of the melting temperature ($\simeq 18K$) obtained from our calculation, we obtain $\chi \simeq 1/450K^{-1}$. If we assume that the density distribution in the crystalline state is represented by a sum of Gaussian density profiles centered at the lattice sites, i.e. $\bar{\rho}(\mathbf{r}) = \sum_i f(\mathbf{r} - \mathbf{R}_i)$, with $f(\mathbf{r}) = \alpha/\pi \exp(-\alpha r^2)$, the assumed form of $\langle u^2 \rangle$ implies that $\alpha(T) = 1/(a_0^2 \chi T)$. The time-averaged Fourier components of the density field are then given by $\rho_{\mathbf{G}} = \exp(-G^2 a_0^2 \chi T/4) = \exp(-4\pi^2(m^2 + n^2 + mn)\chi T/3)$. The second moment of the local field distribution is calculated using

$$[\Delta B^2] = B_0^2 \sum_{\mathbf{G} \neq 0} \frac{w^2(G) K_1^2(w(G)) \rho_{\mathbf{G}} \rho_{-\mathbf{G}}}{(1 + \lambda^2 G^2)^2}. \quad (4.3)$$

The temperature dependence of the second moment comes from two sources – the (assumed two-fluid) temperature dependence of λ on T , as well as the temperature dependence of the $\rho_{\mathbf{G}}$ s. Fig. 8 shows the temperature dependence of the second moment as calculated in this approximation. Note the curvature of the plot of $(\Delta B)^2$ vs. T . This trend is *opposite* to that obtained if one assumes a two-fluid form for the T -dependence of λ and ignores the corrections arising from the temperature-dependence of the broadening of the density distribution. A similar trend is seen in some experiments [13] at not too high fields ($B_0 < 1.5$ T). While the use of Debye-Waller-like broadening factors to rationalize the non-two-fluid temperature dependence of $[\Delta B^2]$ is not new (see [13,30]), in our calculation, these factors are not obtained as fitting parameters but follow from the general structure of our theory.

In Fig. 9, we show the temperature dependence of the third moment, as obtained in this calculation using

$$[\Delta B^3] = B_0^3 \sum_{\substack{\mathbf{G}_1, \mathbf{G}_2, \mathbf{G}_3 \neq 0 \\ \mathbf{G}_1 + \mathbf{G}_2 + \mathbf{G}_3 = 0}} \frac{\sigma(G_1)\sigma(G_2)\sigma(G_3)\rho_{\mathbf{G}_1}\rho_{\mathbf{G}_2}\rho_{\mathbf{G}_3}}{(1 + \lambda^2 G_1^2)(1 + \lambda^2 G_2^2)(1 + \lambda^2 G_3^2)}, \quad (4.4)$$

where $\sigma(G_i)$, $i = 1, 2, 3$ represent the cutoff correction described in section II (see Eq.(2.14)).

The results of our replica treatment [41] of the effects of weak pinning disorder on the correlations and freezing of the vortex system indicate that the results obtained above for the pure system would remain essentially unchanged if the low-temperature “solid” state in the presence of pinning exhibits strong local crystalline order. As discussed in section IIIC above, the freezing of the liquid into such a state may be described by a density functional (see Eq.(3.13)) in which the quantity $[C^{(1)}(\mathbf{r}) - C^{(2)}(\mathbf{r})]$ plays the same role as that of the direct correlation function $C(\mathbf{r})$ in the density functional theory of freezing of the pure system. Our replica liquid state theory [41] shows that if the pinning disorder is weak, then the function $C^{(1)}(\mathbf{r})$ is nearly identical to the function $C(\mathbf{r})$ for the pure system, and $C^{(2)}(\mathbf{r})$ is much smaller, so that $C^{(1)}(\mathbf{r}) - C^{(2)}(\mathbf{r}) \simeq C(\mathbf{r})$. This, in turn, implies that the $\rho_{\mathbf{G}}$ s that describe the (local) density distribution in the low-temperature state in the presence of pinning are nearly the same as those obtained for the pure system. Since the μ SR spectrum in the low-temperature state is determined by the values of the $\rho_{\mathbf{G}}$ s (see Eqs. (4.3) and (4.4)), it would be nearly unaffected by pinning disorder as long as the approximation of describing the local translational order in the low-temperature state by the $\rho_{\mathbf{G}}$ s remains valid. This is expected because, as discussed earlier, μ SR spectroscopy probes the *local* translational order of the vortex system.

Before we conclude this section, we comment briefly on the liquid-solid phase boundary obtained in our calculation in relation to the experimental data. Our calculations, using a Rogers-Young closure scheme and a one-parameter density functional theory, indicate that the liquid-solid phase boundary in the pure system at high fields is practically independent of field and occurs at $T_M \simeq 18K$. This value is slightly lower than the values obtained in experiments [6,7]. In our calculations, we used values of $\lambda_{ab} = 1500-1800\text{\AA}$. Assuming larger values of λ_{ab} would act to shift the phase boundary to still lower temperatures. However, as we have argued earlier [36], the principal source of error in our estimation of the phase

boundary arises from the fact that our liquid state approximations *underestimate* correlations in the liquid. A more accurate treatment of liquid state correlations is expected to shift the phase boundary to higher temperatures. Also, a comparison of our results for the pure system at high fields with the experimental data may not be particularly meaningful because, as discussed in section I above, the freezing observed in experiments at high fields is probably to a glassy state rather than to a crystalline one.

V. μ SR SPECTRUM IN A “FROZEN” LIQUID

We now discuss the calculation of the moments of $n(B)$ in the liquid phase of the vortex system. If the time scale of structural relaxation in the liquid (i.e. the time scale over which the local density becomes homogeneous in the pure system, or nearly homogeneous if weak pinning is present) is much smaller than the inverse muon precession rate, the density distribution seen by the muons should be nearly homogeneous and the line widths vanishingly small. In the opposite limit, in which structural relaxation in the liquid occurs over times that are much longer than the inverse muon precession rate and the muon lifetime, some quantitative progress may be made in calculating μ SR lineshapes and linewidths. We propose that such a limit is appropriate for a description of the low-temperature, high-field state of the flux line ensemble in BSCCO. Such glassy behavior may have several origins, as discussed in the Introduction. Irrespective of the precise nature of this state, it is a reasonable guess that it exhibits short range positional correlations but no long range crystalline order. A natural assumption then, is that positional correlations in this state should resemble those in a liquid. As mentioned in the Introduction, this proposal is consistent with existing neutron scattering [20] and other experimental data. It is also physically sensible, as it provides a way by which some degree of local correlations can be built into the glassy state, while ensuring that crystalline long-range order is destroyed, as required by the Larkin-Ovchinnikov argument [42]. In this section, we explore the consequences of this proposal.

In this (adiabatic) limit, the muons essentially see a “snapshot” of the liquid (i.e. a

typical liquid-like configuration of the pancake vortices). The second moment of the field distribution function is then given by the *space-averaged* two-point correlation function of the density in the configuration seen by the muons. If the system is self-averaging (we assume that it is so), then this correlation function is nothing but the *time-averaged* (equilibrium) two-point density correlation function of the liquid. Therefore, the linewidth in this limit can be calculated in terms of the static structure factor $S(k)$ of the liquid, which is defined as

$$S(\mathbf{k}) = \frac{1}{N} \langle \rho_{\mathbf{k}} \rho_{-\mathbf{k}} \rangle = 1 + \frac{1}{N} \langle \sum_{i \neq j} \exp(i\mathbf{k} \cdot \mathbf{r}_{ij}) \rangle, \quad (5.1)$$

where $\mathbf{r}_{ij} = \mathbf{r}_i - \mathbf{r}_j$ (\mathbf{r}_i is the position vector of the i th pancake vortex), N is the total number of vortices, the sum runs over all the vortices, and the brackets $\langle \dots \rangle$ denote a thermal average. The second moment of the field distribution function is given by

$$[\Delta B^2] = [\Delta B_{\perp}^2] + [\Delta B_z^2]. \quad (5.2)$$

The brackets $[\dots]$ denote a space average for a typical liquid-like configuration of the vortex system. Precisely which moment ($[\Delta B_z^2]$ or $[\Delta B_{\perp}^2]$) is measured depends on the geometry in which the experiments are done. Our results are illustrated here for the transverse μ SR geometry, in which the muons are injected with their polarizations in the plane of the superconducting layers and thus perpendicular to the external field. In this geometry, the measured quantity is $[\Delta B_z^2]$.

The equivalence of space and thermal averages then leads to the following expression for the second moment of the distribution of B_z :

$$[\Delta B_z^2] = \frac{\rho_{\ell}}{d} \frac{1}{(2\pi)^3} \int d^2 k_{\perp} dk_z b_z^2(k_{\perp}, k_z) S(k_{\perp}, k_z), \quad (5.3)$$

where $\rho_{\ell} \equiv B_0/\Phi_0$ denotes the (areal) density of vortices, and the quantity b_z is defined in Eq.(3.3). A similar expression for $[\Delta B_{\perp}^2]$ may be obtained by replacing b_z by b_{\perp} (see Eq.(3.2)) in the above equation.

Before analyzing the relevance of short-range correlations in the computation of moments of $n(B)$ in the frozen liquid, we discuss two simple limiting cases. First consider the limit in

which the liquid has *no* correlations, so that $S(k_\perp, k_z) = 1$, and the second moment of the distribution of the z -component of the field is given by

$$[\Delta B_z^2] = \frac{\rho_\ell \Phi_0^2 d^2}{d (2\pi)^2} \int_0^\infty k_\perp dk_\perp \int_{-\infty}^\infty \frac{dk_z}{(1 + \lambda^2 k_\perp^2 + \lambda^2 k_z^2)^2} = B_0 \Phi_0 d / 8\pi \lambda^3. \quad (5.4)$$

For $B = 0.5\text{T}$, $d = 15\text{\AA}$ and $\lambda = 1500\text{\AA}$, we obtain $[\Delta B_z^2] = 1830 \text{ G}^2$, whereas assuming $\lambda = 1800\text{\AA}$ gives $[\Delta B_z^2] = 1059 \text{ G}^2$.

Now consider the case of a completely uncorrelated arrangement of rigid flux lines. The second moment of the field distribution is then given by

$$[\Delta B_z^2] = \frac{\rho_\ell}{(2\pi)^2} \int \frac{\Phi_0^2}{(1 + \lambda^2 k_\perp^2)^2} d^2 k_\perp = \frac{B_0 \Phi_0}{4\pi \lambda^2}. \quad (5.5)$$

Assuming, as before, $B_0 = 0.5\text{T}$ and $\lambda = 1500\text{\AA}$, we obtain $[\Delta B_z^2] = 3.66 \times 10^5 \text{ G}^2$ ($2.54 \times 10^5 \text{ G}^2$ for $\lambda = 1800\text{\AA}$). These numbers are to be compared with the value of $[\Delta B_z^2]$ ($= 3140 \text{ G}^2$ for $\lambda = 1500\text{\AA}$, 1514 G^2 for $\lambda = 1800\text{\AA}$) for a perfect Abrikosov lattice.

These simple results, first derived by Brandt [54], bring out an important point: the destruction of correlations in the ab -plane (while keeping the vortices perfectly correlated in the c -direction) greatly *increases* the linewidth, whereas the destruction of correlations in the c -direction causes the linewidth to become smaller. This observation suggests that a likely candidate for a structure that exhibits anomalously narrow μSR linewidths would be one with at least local (see below) positional correlations in the layer planes and little correlation across the layers. Our proposal for the structure of the “glassy” state of the vortex system is consistent with this expectation: our liquid state calculations [35,36] show that the equilibrium liquid just above freezing exhibits pronounced short-range correlations in the layer plane, but the correlation length in the c -direction remains small (about 15 – 20 layer spacings).

We now describe a simple calculation that illustrates that the presence of *short-range* ab -plane correlations in a frozen liquid of rigid flux lines is sufficient to bring down the linewidth to values comparable to that obtained for a perfect Abrikosov lattice. The inclusion of local correlations in the calculation of the moments of the field distribution

requires the specification of the liquid structure factor $S(k_\perp)$. At the simplest level, $S(k_\perp)$ can be approximated as

$$\begin{aligned} S(k_\perp) &= 0 & (0 < k_\perp < k_m - \epsilon), \\ &= S_m & (k_m - \epsilon < k_\perp < k_m + \epsilon), \\ &= 1 & (k_m + \epsilon < k_\perp < \infty). \end{aligned} \quad (5.6)$$

This approximation retains all the basic qualitative features expected of a fluid structure factor – it rises from a value of zero near the origin of k -space to a peak at a k -space distance of the order of 2π times the inverse of the mean interparticle spacing, and becomes unity at sufficiently large k . With this approximation, it is easy to obtain

$$[\Delta B_z^2] = \frac{B\Phi_0}{2\pi\lambda^4} \left(\frac{2\epsilon S_m}{k_m^3} + \frac{1}{2k_m^2} \right). \quad (5.7)$$

Assuming $2\epsilon S_m/k_m \sim 0.5$, so that $[\Delta B_z^2] \simeq B\Phi_0/(2\pi\lambda^4 k_m^2)$, $k_m^2 \simeq 4\pi^2 B/\Phi_0$, and for sufficiently large fields (so that $(1 + \lambda^2 k_m^2) \simeq \lambda^2 k_m^2$), we obtain

$$[\Delta B_z^2] \simeq \frac{\Phi_0^2}{8\pi^3\lambda^4} \simeq 4 \times 10^{-3} \frac{\Phi_0^2}{\lambda^4}, \quad (5.8)$$

which is quite close to the result, $[\Delta B_z^2] \simeq 3.71 \times 10^{-3} \frac{\Phi_0^2}{\lambda^4}$, for the linewidth in a perfect Abrikosov lattice. This admittedly crude calculation thus brings out the important point that the μ SR linewidth is sensitive only to the *local* order.

We now proceed to describe our detailed calculation of the linewidths in a frozen liquid-like state. In terms of the direct correlation function, Eq.(5.3) can be written as

$$[\Delta B_z^2] = \frac{\rho_\ell}{d} \frac{1}{(2\pi)^2} \int_0^\infty k_\perp dk_\perp \int_{-\infty}^\infty dk_z \frac{\phi_0^2 d^2}{(1 + \lambda^2 k_\perp^2 + \lambda^2 k_z^2)^2} \frac{1}{(1 - \rho_\ell C(k_\perp, k_z))}, \quad (5.9)$$

where $C(k_\perp, k_z)$ is the liquid direct correlation function and we have used the relation $S(k_\perp, k_z) = 1/(1 - \rho_\ell C(k_\perp, k_z))$. The direct correlation function $C(k_\perp, k_z)$ is obtained from our earlier calculation [35,36] of the equal-time correlations in a layered vortex liquid. To represent the core form factors (in order to reduce the complexity of the expressions, we do not explicitly show these form factors in the equations derived below), we model the core of

a pancake vortex as a cylinder of radial dimension $\xi_{ab} \simeq 15\text{\AA}$ and height $\xi_c \simeq 3\text{\AA}$. We use the decomposition

$$C(\rho, nd) = C_s(\rho, nd) + C_L(\rho, nd), \quad (5.10)$$

where the ‘‘long-range’’ part of C is given by $C_L(\rho, nd) = -\beta V(\rho, nd)$ ($V(\rho, nd)$, the inter-vortex interaction in position space, is the Fourier transform of $V(\mathbf{k})$ defined in Eq.(3.1)). Asymptotically, $C(\rho, nd)$ tends to the value $-\beta V(\rho, nd)$, which we have called $C_L(\rho, nd)$, so that $C_s(\rho, nd)$ tends to zero. This ‘‘short-range’’ part is assumed to have the form $C_s(\rho, nd) = C_s(\rho, n = 0)\delta_{n,0}$ (see [35,36]). The Fourier transform, $C_s(k_\perp)$, of the function $C_s(\rho, n = 0)$ is obtained by numerically solving the self-consistent equations of liquid state theory. Approximating $\sin^2(k_z d/2)$ appearing in Eq.(3.1) by $k_z^2 d^2/4$, the integral over k_z in Eq.(5.9) can be performed to yield

$$[\Delta B_z^2] = \frac{\Phi_0^2 d}{4\pi\Gamma\lambda^2} \int_0^\infty dk_\perp k_\perp^3 \left(\sqrt{\frac{Y}{X}} - \sqrt{\frac{\lambda^2}{1 + \lambda^2 k_\perp^2}} \right), \quad (5.11)$$

where

$$\begin{aligned} X &= k_\perp^2 (1 + \lambda^2 k_\perp^2) (1 - \rho_\ell C_s(k_\perp)) + \rho_\ell \Gamma \lambda^2 k_\perp^2, \\ Y &= \lambda^2 k_\perp^2 (1 - \rho_\ell C_s(k_\perp)) + \rho_\ell \Gamma \lambda^2. \end{aligned} \quad (5.12)$$

These equations and the numerically obtained $C_s(k_\perp)$ are used to evaluate the second moment $[\Delta B_z^2]$.

The third moment of the field distribution function in the liquid phase can be obtained via the liquid state methods we have discussed here, together with a simple decoupling approximation. Using

$$[\Delta B_z^3] = \frac{1}{V^3} \sum_{\mathbf{k}_1, \mathbf{k}_2, \mathbf{k}_3} \langle \rho(\mathbf{k}_1) \rho(\mathbf{k}_2) \rho(-\mathbf{k}_1 - \mathbf{k}_2) \rangle b_z(\mathbf{k}_1) b_z(\mathbf{k}_2) b_z(-\mathbf{k}_1 - \mathbf{k}_2), \quad (5.13)$$

what is required to calculate this moment is the triplet structure factor $S^{(3)}(\mathbf{k}_1, \mathbf{k}_2)$ defined by

$$S^{(3)}(\mathbf{k}_1, \mathbf{k}_2) = \frac{1}{N} \langle \rho(\mathbf{k}_1) \rho(\mathbf{k}_2) \rho(-\mathbf{k}_1 - \mathbf{k}_2) \rangle. \quad (5.14)$$

In terms of the triplet direct correlation function $C^3(\mathbf{k}_1, \mathbf{k}_2)$, this assumes the form

$$C^3(\mathbf{k}_1, \mathbf{k}_2) = 1 - \frac{S^{(3)}(\mathbf{k}_1, \mathbf{k}_2)}{S(\mathbf{k}_1)S(\mathbf{k}_2)S(-\mathbf{k}_1 - \mathbf{k}_2)}. \quad (5.15)$$

The triplet correlation function is typically small in magnitude in regular three dimensional solids. If it is assumed to be zero, (the so-called convolution relation [55]), the integral can be written completely in terms of the the static structure factor. We thus obtain

$$[\Delta B_z^3] = \frac{\rho \ell}{d} \frac{1}{(2\pi)^6} \int d\mathbf{k}_{1\perp} \int dk_{1z} \int d\mathbf{k}_{2\perp} \int dk_{2z} S(\mathbf{k}_1)S(\mathbf{k}_2)S(-\mathbf{k}_1 - \mathbf{k}_2)b_z(\mathbf{k}_1)b_z(\mathbf{k}_2)b_z(-\mathbf{k}_1 - \mathbf{k}_2). \quad (5.16)$$

This expression is defined in terms of the two-particle structure factor $S(k_\perp, k_z)$ which, as discussed above, may be obtained from the function $C_s(k_\perp)$ calculated in our liquid state theory. Exploiting the structure of this expression, and after considerable algebra, the 6-dimensional integral is reduced to a 3-dimensional one which is evaluated numerically.

Our results for $[\Delta B_z^2]$ and $[\Delta B_z^3]$ for values of $\lambda_{ab} = 1500\text{\AA}$ and 1800\AA are summarized in Table I. These results are obtained using the $C_s(k_\perp)$ calculated just above the melting transition. The core form factors, omitted for simplicity in the expressions derived above, are present in the full calculation. While our liquid-state calculations are performed for $\lambda = 1500\text{\AA}$, the calculated $C_s(k_\perp)$ can be used for the case $\lambda_{ab} = 1800\text{\AA}$ in the high field limit provided the melting temperature is scaled as $T_M \propto 1/\lambda_{ab}^2$. This is a simple consequence of the crossover to quasi-two-dimensional behavior at high fields, in which the dominant interaction is the (scale-invariant) logarithmic coupling between vortices on the same plane, which is perturbed only weakly by the presence of vortices on other planes. Comparison with experimental data [17] shows that our proposal agrees quite well with the results of experiments.

Results for $[\Delta B_\perp^2]$ can be obtained from

$$[\Delta B_\perp^2] = \frac{\Phi_0^2 d}{4\pi\Gamma\lambda^2} \int_0^\infty dk_\perp k_\perp \left[\sqrt{\frac{1 + \lambda^2 k_\perp^2}{\lambda^2}} - \sqrt{\frac{X}{Y}} \right]. \quad (5.17)$$

Here X and Y are as defined in Eq.(5.12). The value of this moment is comparable to $[\Delta B_z^2]$.

Our *ansatz* that the vortices remain stationary during the lifetime (or precession time if it is smaller) of the muons is expected to be strictly valid only at very low temperatures – at higher temperatures we would expect the effects of thermal broadening of the (now inhomogeneous) density distributions to *reduce* linewidths further in analogy with our results for the crystalline phase in the pure system. There seems to be no simple way of incorporating such thermal effects into the theory described here (see, however, the discussion in section VII below). A theoretical investigation of the temperature dependence of the linewidth in this disordered phase would be interesting. It would also be worthwhile to carry out a more accurate calculation of the third moment of the field distribution by going beyond the simple decoupling approximation used here.

In the calculations described above, we used the equilibrium correlation function of the *pure* liquid at a temperature just above the crystallization temperature T_M to determine the moments of the field distribution. Since the glassy phase we are interested in is expected to arise as a consequence of the presence of pinning disorder, one should, in principle, use the correlation function of the disordered liquid near its freezing (glass transition) temperature in these calculations. Due to reasons mentioned below, we expect that the results of such a calculation would be essentially the same as those described above. Our replica calculation [41] of liquid state correlations in the presence of pinning disorder shows that the equal-time (equilibrium) density correlations in the liquid are basically unaffected by weak disorder. Therefore, our approximation of replacing the static structure factor of the disordered liquid by that of the pure one is expected to be quite accurate. We also find that the value of the linewidth depends relatively weakly on the temperature at which the liquid-state correlations are calculated – a change in the temperature from T_M to $3T_M$ leads to a decrease of about 20% in the linewidth $[\Delta B^2]$. This observation indicates that a small difference between T_M and the actual glass transition temperature of the disordered liquid would not cause any significant change in the final results.

VI. μ SR LINEWIDTH IN THE DISORDERED LIQUID

The time scales for structural relaxation in the high-temperature liquid phase are expected to be short. The second moment of the field distribution function in this phase of the pure system would be vanishingly small if these time scales are fast compared to the inverse precession rate of the muons. Even in this limit, however, measurable line-widths can obtain in the presence of quenched pinning disorder. The source of this broadening is the off-diagonal (in replica space) density correlation function. Off-diagonal correlations, which are absent in the pure system, become non-zero in the presence of disorder. These correlations arise due to the disorder-induced inhomogeneity of the time-averaged local density. In a replica symmetric description, the off-diagonal radial distribution function is defined as

$$g^{(2)}(\mathbf{r}) \equiv \langle\langle \rho^\alpha(0)\rho^{\beta\neq\alpha}(\mathbf{r}) \rangle\rangle / \rho_\ell^2 = [\langle\rho(0)\rangle\langle\rho(\mathbf{r})\rangle] / \rho_\ell^2. \quad (6.1)$$

Here the ρ s represent local number densities, α and β are replica indices, $\langle\langle \dots \rangle\rangle$ represents an average over the canonical distribution function of the replicated system and $\langle \dots \rangle$, a thermal average for the original disordered system prior to averaging over disorder. The square brackets $[\dots]$ denote an average over the probability distribution governing the disorder.

If the relaxation times of the liquid are short, then the muons see the time-averaged (equilibrium) density distribution which is inhomogeneous if pinning disorder is present. In this case, the second moment of the field distribution function can be obtained from the correlation function $h^{(2)} \equiv g^{(2)} - 1$ that describes the correlation of the deviations of the time-averaged local density from its space-averaged value ρ_ℓ . Specifically, the second moment of the distribution of the z -component of the local magnetic field is given by

$$[\Delta B_z^2] = \frac{\rho_\ell}{d} \frac{1}{(2\pi)^3} \int d\mathbf{k}_\perp \int dk_z b_z^2 S^{(2)}(k_\perp, k_z), \quad (6.2)$$

where $S^{(2)}(\mathbf{k})$, the off-diagonal structure factor defined as $[\langle\delta\rho_{\mathbf{k}}\rangle\langle\delta\rho_{-\mathbf{k}}\rangle]/N$, is given by (see Eq.(3.11))

$$S^{(2)}(\mathbf{k}) = \rho_\ell h^{(2)}(\mathbf{k}) = \frac{\rho_\ell C^{(2)}(\mathbf{k})}{[1 - \rho_\ell C^{(1)}(\mathbf{k}) + \rho_\ell C^{(2)}(\mathbf{k})]^2}. \quad (6.3)$$

Using this and the expression, Eq.(3.3), for b_z , Eq.(6.2) can be written as

$$[\Delta B_z^2] = \frac{\rho_\ell}{d} \frac{1}{(2\pi)^3} \int d\mathbf{k}_\perp \int dk_z \frac{\Phi_0^2 d^2}{(1 + \lambda^2 k_\perp^2 + \lambda^2 k_z^2)^2} \frac{\rho_\ell C^{(2)}(k_\perp, k_z)}{[1 - \rho_\ell C^{(1)}(k_\perp, k_z) + \rho_\ell C^{(2)}(k_\perp, k_z)]^2}. \quad (6.4)$$

Separating the diagonal direct correlation function $C^{(1)}$ as before into a short-range and a long-range part and evaluating the integral over k_z , we get

$$[\Delta B_z^2] = \frac{\rho_\ell \Phi_0^2 d^2}{d} \frac{1}{8\pi} \int_0^\infty k_\perp dk_\perp \rho_\ell C^{(2)}(k_\perp) \frac{1}{\sqrt{P}Q^{3/2}}, \quad (6.5)$$

where P and Q are given by

$$\begin{aligned} P &= (1 + \lambda^2 k_\perp^2)(1 - \rho_\ell C_s^{(1)}(k_\perp) + \rho_\ell C^{(2)}(k_\perp)) + \rho_\ell \Gamma \lambda^2, \\ Q &= \lambda^2(1 - \rho_\ell C_s^{(1)}(k_\perp) + \rho_\ell C^{(2)}(k_\perp)) + \frac{\rho_\ell \Gamma \lambda^2}{k_\perp^2}. \end{aligned} \quad (6.6)$$

In deriving the above equation, we have used the approximation $C^{(2)}(\rho, nd) = C^{(2)}(\rho)\delta_{n,0}$, so that its Fourier transform $C^{(2)}(k_\perp, k_z)$ does not depend on k_z . This approximation is justified [41] because the interaction between different replicas (Eq.(3.12)) does not couple vortices on different layers.

Evaluating the integral in Eq.(6.5) numerically, using the values for $C^{(1)}$ and $C^{(2)}$ obtained in Ref. [41] through a self-consistent solution of the replicated liquid state equations, we obtain values for $[\Delta B_z^2]$ in the range $1 - 10G^2$. At $B_0 = 0.3$ T, just above the melting transition, our calculations yield $[\Delta B_z^2] = 4.7G^2$. The smallness of this number reflects the numerically small value of $C^{(2)}(k_\perp)$. Further, this quantity vanishes as the off-diagonal coupling (equivalently, the disorder strength) is reduced to zero, leading to the expected vanishing of the linewidth in the high-temperature liquid phase of the pure system. The relatively strong dependence of $C^{(2)}$ on the disorder strength suggests that the linewidths obtained in the liquid phase at high temperatures should increase as the sample is progressively made more disordered.

VII. SUMMARY AND DISCUSSION

In this paper we have presented a theory for μ SR spectra in anisotropic, layered superconductors which incorporates thermal effects in both the solid and the liquid phase, and the

effects of weak pinning disorder. In particular, we have computed the effects of thermal fluctuations and disorder in determining the μ SR linewidths and lineshapes in the mixed phase of the extensively studied high-temperature superconductor BSCCO. In the crystalline solid phase, our density functional description of the time-averaged density distribution offers a *nonperturbative* way of assessing the effects of thermal broadening. Our theory of μ SR spectra in the liquid phase represents, to the best of our knowledge, the first attempt to calculate linewidths in this phase beyond the simplest assumption of uncorrelated lines or vortices. Our analysis suggests that the experimentally obtained linewidths in the low-temperature, high-field state in BSCCO may be understood if one assumes that vortices in this regime are in a frozen state that resembles a liquid in its local correlations. We have also quantified the effects of pinning disorder on the μ SR linewidth in the high-temperature vortex liquid. The results of our calculations are in qualitative (quantitative in some cases) agreement with those obtained in experiments on BSCCO.

An *implicit* assumption we have made is that the flux-lattice can be treated classically, i.e. the characteristic temperature below which quantum effects are non-negligible lies far below the equilibrium melting temperature. This assumption has been questioned recently by Bulaevskii et al. [48] who argue that quantum effects are non-negligible except at temperatures close to the superconducting transition temperature $T_c(0)$. Their argument rests on the assumption that the characteristic energy scale for quantum effects is set by the superconducting gap and therefore is $\sim k_B T_c(0)$. While much is still to be understood about the precise role of quantum effects in the mixed phase, we believe that the success of the density functional approach in describing flux-lattice melting (which assumes that a classical liquid state description can be used in treating the liquid) serves as a counter example to the assertion that quantum effects must be included in any theory for the mixed phase. As we have emphasized, our theory yields a value of the freezing temperature that is lower than the experimentally observed value – quantum effects would surely act to depress this value further.

Our results for the effects of pinning disorder on the μ SR spectrum are based on the

replica liquid state theory developed in Ref. [41] where only replica symmetric solutions of the liquid state equations were considered. A recent study [56] of the same set of equations for simple isotropic liquids shows that these equations exhibit a replica symmetry breaking transition which may be interpreted as a glass transition. This work suggests that the low-temperature, high-field state of BSCCO may correspond to a replica symmetry broken solution of the liquid state equations derived in Ref. [41]. In Ref. [56], the two-point correlation function of the “frozen” local density in the glassy phase is found to be quite similar to the equal-time (equilibrium) correlation function of the local density in the liquid phase. This observation supports the *ansatz* we have used in this paper for the structure of the low-temperature, high-field state of BSCCO.

Acknowledgements:

One of us (GIM) is grateful for support from NSERC of Canada.

REFERENCES

- [†] Present and permanent address: The Institute of Mathematical Sciences, C.I.T. Campus, Taramani, Chennai - 600113, India.
- [‡] Also at the Condensed Matter Theory Unit, Jawaharlal Nehru Centre for Advanced Scientific Research, Bangalore - 560064, India.
- [1] A. A. Abrikosov, *Zh. Eksp. Teor. Fiz* **32**, 1442 (1957).
- [2] A. Schenck, *Muon Spin Rotation Spectroscopy: Principles and Applications in Solid State Physics* (Adam Hilger Ltd., Bristol and Boston, 1985.)
- [3] E. H. Brandt and A. Seeger, *Adv. Phys* **35**, 189 (1986).
- [4] Yu. M. Belousov, V.N. Gorbunov, V.P. Smilga and V.I. Fesenko, *Sov. Phys. Usp.* **33**, 911 (1990).
- [5] For a review of flux-lattice melting, see G. Blatter, M.V. Feigel'man, V.B. Geshkenbein, A.I. Larkin and V.M. Vinokur, *Rev. Mod. Phys.* **66**, 1125 (1995).
- [6] S. L. Lee, P. Zimmermann, H. Keller, M. Warden, I.M. Savic, R. Schauwecker, D. Zech, R. Cubitt, E.M. Forgan, P.H. Kes, T.W. Li, A.A. Menovsky and Z. Tarnawski, *Phys. Rev. Lett.* **71**, 3862 (1993).
- [7] S. L. Lee, M. Warden, H. Keller, J.W. Schneider, D. Zech, P. Zimmermann, R. Cubitt, E.M. Forgan, M.T. Wylie, P.H. Kes, T.W. Li, A.A. Menovsky and Z. Tarnawski, *Phys. Rev. Lett.* **75**, 922 (1995).
- [8] S. L. Lee, A.M. Aegerter, H. Keller, M. Willemin, B. Stauble-Pumpin, E.M. Forgan, S.H. Lloyd, G. Blatter, R. Cubitt, T.W. Li and P.H. Kes, *Phys. Rev. B* **55**, 5666 (1997).
- [9] J. E. Sonier, R.F. Kiefl, J.H. Brewer, D.A. Bonn, J.F. Carolan, K.H. Chow, P. Dosanjh, W.N. Hardy, Ruixing Liang, W.A. MacFarlane, P. Mendels, G.D. Morris, T.M. Riseman and J.W. Schneider, *Phys. Rev. Lett.* **72**, 744 (1994).

- [10] T. M. Riseman, J.H. Brewer, K.H. Chow, W.N. Hardy, R.F. Kiefl, S.R. Kreitzman, R. Liang, W.A. MacFarlane, P. Mendels, G.D. Morris, J. Rammer, J.W. Schneider, C. Niedermayer, S.L. Lee, Phys. Rev. B **52**, 10569 (1995).
- [11] J. E. Sonier, R.F. Kiefl, J.H. Brewer, D.A. Bonn, S.R. Dunsiger, W.N. Hardy, Ruixing Liang, W.A. MacFarlane, T.M. Riseman, D.R. Noakes, and C.E. Stronach, Phys. Rev. B **55**, 11789 (1997).
- [12] H. Keller, W. Kundig, I.M. Savic, H. Simmler, B. Stauble-Pumpin, M. Warden, D. Zech, P. Zimmermann, E. Kaldis, J. Karpinski, S. Rusiecki, J.H. Brewer, T.M. Riseman, J.W. Schneider, Y. Maeno and C. Rossel, Physica C **185-189**, 1089 (1991).
- [13] D. R. Harshman, R.N. Kleiman, M. Inui, G.P. Espinoza, D.B. Mitzi, A. Kapitulnik, T. Pfiz, and D. Ll. Williams, Phys. Rev. Lett. **67**, 3152 (1991).
- [14] T. Schneider, Z. Phys. B - Cond. Mat. **88**, 249 (1992).
- [15] C. Bernhard, C. Wenger, Ch. Niedermayer, D.M. Pooke, J.L. Tallon, Y. Kotaka, J. Shimoyama, K. Kishio, D.R. Noakes, C.E. Stronach, T. Sembring, E.J. Ansaldo, Phys. Rev. B **52**, R7050 (1995).
- [16] C. M. Aegerter, S.L. Lee, H. Keller, E.M. Forgan and S.H. Lloyd, Phys. Rev. B **54**, R15661 (1996).
- [17] μ SR spectra for BSCCO crystals at 5 K show, for $B_0 = 0.3, 0.4$ and 1.5 T respectively, squared linewidth values of $[\Delta B^2] = 90 \pm 4, 80 \pm 5,$ and $52 \pm 8 \text{ G}^2$ and third moments of $[\Delta B^3] = 1000 \pm 80, 500 \pm 100$ and $0 \pm 250 \text{ G}^3$ [13,30].
- [18] J. H. Cho *et al.*, Phys. Rev. B **50**, 6493 (1994), and references therein.
- [19] B. Khaykovich, E. Zeldov, D. Majer, T.W. Li, P.H. Kes and M. Konczykowski, Phys. Rev. Lett. **76**, 2555 (1996), and references therein.
- [20] R. Cubitt, E.M. Forgan, G. Yang, S.L. Lee, D.M. Paul, H.A. Mook, M. Yethiraj, P.H.

- Kes, T.W. Li, A.A. Menovsky and Z. Tarnawski, *Nature* **365**, 407 (1993).
- [21] L. I. Glazman and A. E. Koshelev, *Phys. Rev. B* **43**, 2835 (1991).
- [22] D. Ertas and D. R. Nelson, *Physica C* **272**, 79 (1996).
- [23] M. C. Marchetti and D. R. Nelson, *Phys. Rev. B* **41**, 1910 (1990).
- [24] T. Giamarchi and P. Le Doussal, *Phys. Rev. B* **52**, 1242 (1995).
- [25] T. Giamarchi and P. Le Doussal, *Phys. Rev. B* **55**, 6577 (1997).
- [26] J. Kierfield, T. Nattermann, and T. Hwa, *Phys. Rev. B* **55**, 626 (1997).
- [27] D. S. Fisher, M. P. A. Fisher and D. A. Huse, *Phys. Rev. B* **43**, 130 (1990).
- [28] see, for example, J. R. Clem, *Phys. Rev. B* **43**, 7837 (1991).
- [29] E. H. Brandt, *Phys. Rev. Lett.* **66**, 3213 (1991).
- [30] D. R. Harshman, E.H. Brandt, A.T. Fiory, M. Inui, D.B. Mitzi, L.F. Schneemeyer and J.V. Waszczak, *Phys. Rev. B* **47**, 2905 (1993).
- [31] S. Ryu, A. Kapitulnik, and S. Doniach, *Phys. Rev. Lett.* **77**, 2300 (1996); A. van Otterlo, R.T. Scalettar and G.T. Zimanyi, *Phys. Rev. Lett.*, **81**, 1497 (1998).
- [32] M. Inui and D. R. Harshman, *Phys. Rev. B* **47**, 12205 (1993).
- [33] T. V. Ramakrishnan and M. Yussouff, *Phys. Rev B* **19**, 2775 (1979). See D. W. Oxtoby in *Liquids, Freezing and the Glass Transition*, ed. J.P. Hansen, D. Levesque and J. Zinn-Justin (North-Holland, Amsterdam, 1990), for a recent review.
- [34] Y. Singh, *Physics Reports* **207**, 351 (1991).
- [35] S. Sengupta, C. Dasgupta, H. R. Krishnamurthy, G. I. Menon and T. V. Ramakrishnan, *Phys. Rev. Lett.* **67**, 3444 (1991).
- [36] G. I. Menon, C. Dasgupta, H. R. Krishnamurthy, T. V. Ramakrishnan and S. Sengupta,

- Phys. Rev. B **54**, 16192 (1996).
- [37] W. E. Lawrence and S. Doniach, in it Proc. XII Int. Conf. on Low Temperature Physics, E. Kanda ed. (Keigaku, Tokyo, 1971).
- [38] E. M. Chudnovsky, Phys. Rev. Lett **65**, 3060 (1990).
- [39] A. Yaouanc, P. Dalmas de Reotier and E. H. Brandt, Phys. Rev. B **55**, 11107 (1997).
- [40] See, for example, P. Koorevaar, P. H. Kes, A. E. Koshelev, and J. Aarts, Phys. Rev. Lett. **72**, 3250 (1994).
- [41] G. I. Menon and C. Dasgupta, Phys. Rev. Lett. **73**, 1023 (1994).
- [42] A. I. Larkin, Zh. Eksp. Teor. Fiz, **58**, 1466 (1970) [Sov. Phys. JETP **31**, 784 (1990)]; A. I. Larkin and Y. N. Ovchinnikov, J. Low Temp. Phys. **34**, 409 (1979).
- [43] Y.-Q Song *et al.*, Phys. Rev. Lett **70**, 3127 (1993); Physica C **241**, 187 (1995).
- [44] H. C. Torrey, Phys. Rev. **104**, 563 (1956).
- [45] J. R. Clem in *Low Temperature Physics – LT14*, edited by M. Krusius and M. Vurio (North Holland, Amsterdam, 1975), Vol 2.
- [46] Z. Hao, J.R. Clem, M.W. McElfresh, L. Civale, A.P. Malozemoff and F. Holtzberg, Phys Rev. B **43**, 2844 (1991).
- [47] M. V. Feigel'man, V. B. Geshkenbein and A. I. Larkin, Physica C **167**, 177 (1990).
- [48] L. N. Bulaevskii, M. P. Maley and I. F. Schegolev, Physica B **197**, 506 (1994).
- [49] J. P. Hansen and I. R. Macdonald, *Theory of Simple Liquids*, (Academic, London, 1986), 2nd edition.
- [50] F. J. Rogers and D. A. Young, Phys. Rev. A **30**, 999 (1984).
- [51] D. R. Nelson and P. Le Doussal, Phys. Rev. B **42**, 10 133 (1990).

- [52] T. V. Ramakrishnan, Phys. Rev. Lett. **48**, 541 (1982).
- [53] B. Khaykovich, M. Konczykowski, E. Zeldov, R.A. Doyle, D. Majer, P.H. Kes and T.W. Li, Phys. Rev. B **56**, R517 (1997).
- [54] E. H. Brandt, Phys. Rev B **37**, 2349 (1988).
- [55] H. W. Jackson and E. Feenberg, Rev. Mod. Phys **34**, 683 (1962); S. Ichimaru, Phys. Rev. A **2**, 494 (1970).
- [56] M. Mezard and G. Parisi, J. Phys. A **29**, 6515 (1996).

TABLES

TABLE I. Summary of our results for $[\Delta B_z^2]$ and $[\Delta B_z^3]$ in a slowly relaxing liquid of pancake vortices just above its equilibrium freezing temperature T_M . The results shown are for $B_0 = 0.3$ T, and two values (1500 Å and 1800 Å) of the ab -plane penetration depth λ . According to our *ansatz* (see text) for the structure of the low-temperature disordered phase found in the high-field mixed-phase regime of BSCCO, these calculated values should correspond to the experimentally observed data in this phase at low temperatures. Experimental μ SR spectra for BSCCO crystals at 5 K show, for $B_0 = 0.3, 0.4$ and 1.5T respectively, squared linewidth values of $[\Delta B^2] = 90 \pm 4, 80 \pm 5$, and 52 ± 8 G² and third moments of $[\Delta B^3] = 1000 \pm 80, 500 \pm 100$ and 0 ± 250 G³ (see Ref. [13,30]).

$\lambda(\text{Å})$	$[\Delta B_z^2]$ (G ²)	$[\Delta B_z^3]$ (G ³)	T_M (calculated)
1500	175.3	4022.0	$\simeq 18$ K
1800	111.9	1117.5	$\simeq 12$ K

FIGURES

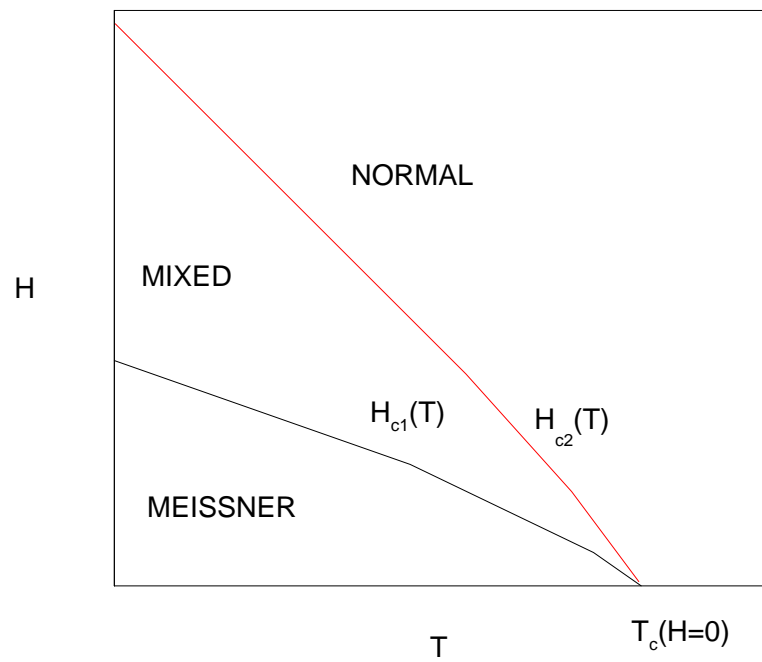


FIG. 1. Schematic $H - T$ phase diagram of a type-II superconductor in mean-field theory, illustrating Meissner, mixed and normal phases separated by continuous phase transitions.

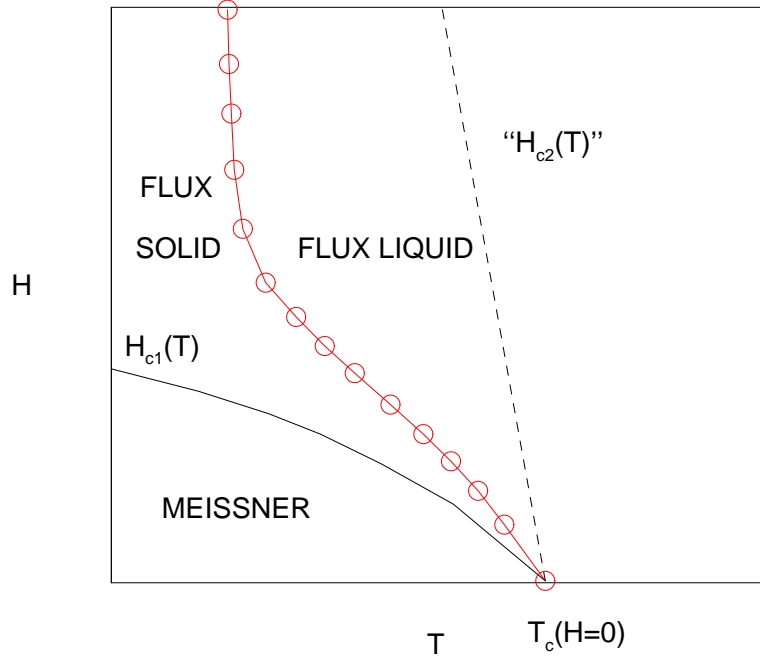


FIG. 2. Schematic $H - T$ phase diagram for pure BSCCO illustrating the effects of thermal fluctuations on the mixed phase. Note the large region of “flux liquid” phase separated from a low-temperature crystalline phase by a first-order liquid-solid phase boundary. A very narrow region of liquid phase expected just above the the H_{c1} line is not shown. The mean-field H_{c2} curve represents a crossover between a regime with strong amplitude fluctuations and one in which amplitude fluctuations are very weak.

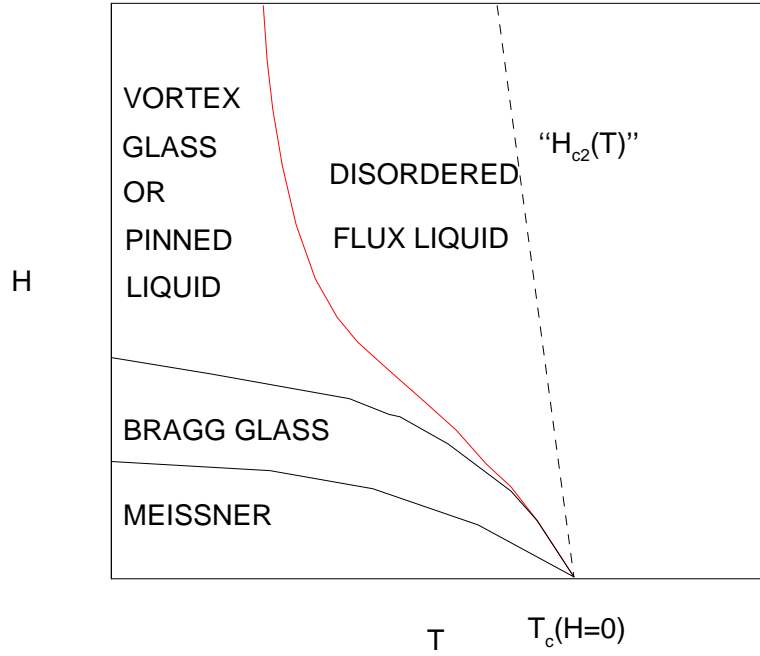


FIG. 3. Schematic phase diagram for BSCCO incorporating effects of thermal fluctuations and quenched disorder due to random point pinning. The phases shown are the “Bragg Glass” phase (I), the “pinned liquid” or “vortex glass” phase (II), the disordered liquid phase (III) and the normal phase (IV). The existence of the Bragg glass and vortex glass phases has not been established conclusively. The boundaries shown between phases (I) and (II) and between phases (II) and (III) may actually correspond to rapid crossovers instead of true phase transitions.

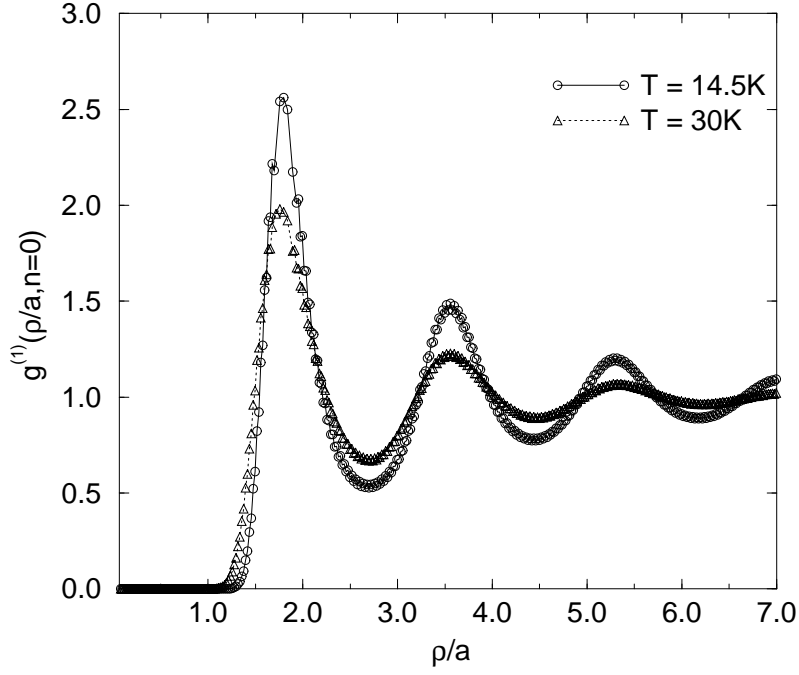


FIG. 4. The diagonal correlation function $g^{(1)}(\rho, n = 0)$, obtained using the formalism described in section IIIC, is plotted as a function of the in-plane separation ρ/a , where a is defined by $\pi a^2 = \Phi_0/B_0$. The results shown are for disorder strength $\Gamma' = 3 \times 10^{-5}\Gamma^2$ (see text for the definitions of Γ and Γ'), $B_0 = 0.3$ T, and $T = 14.5$ K and 30 K.

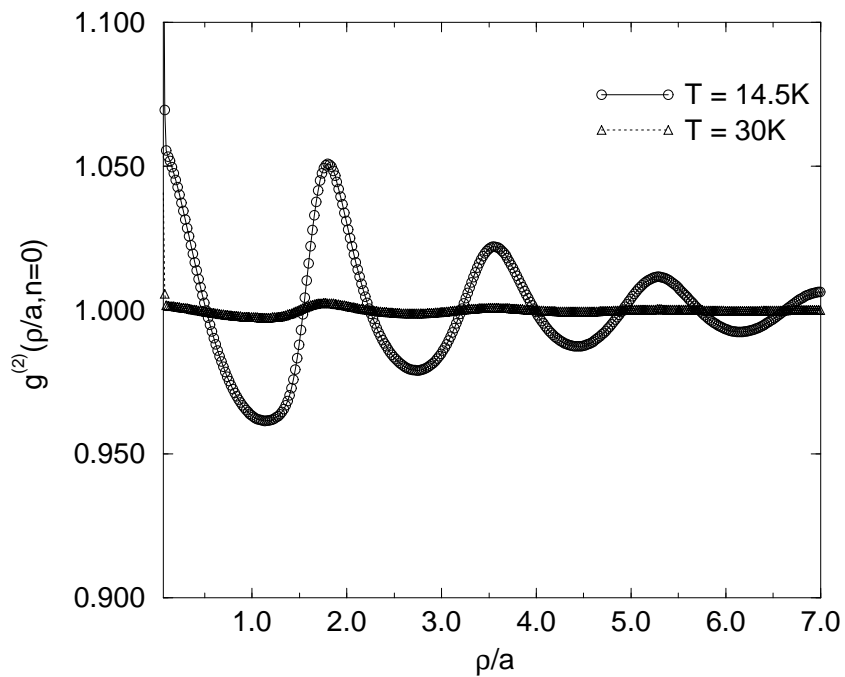


FIG. 5. The off-diagonal correlation function $g^{(2)}(\rho, n = 0)$, obtained using the formalism described in section IIIC, is plotted as a function of the in-plane separation ρ/a , where a is defined by $\pi a^2 = \Phi_0/B_0$. The parameter values are the same as those in Fig. 4.

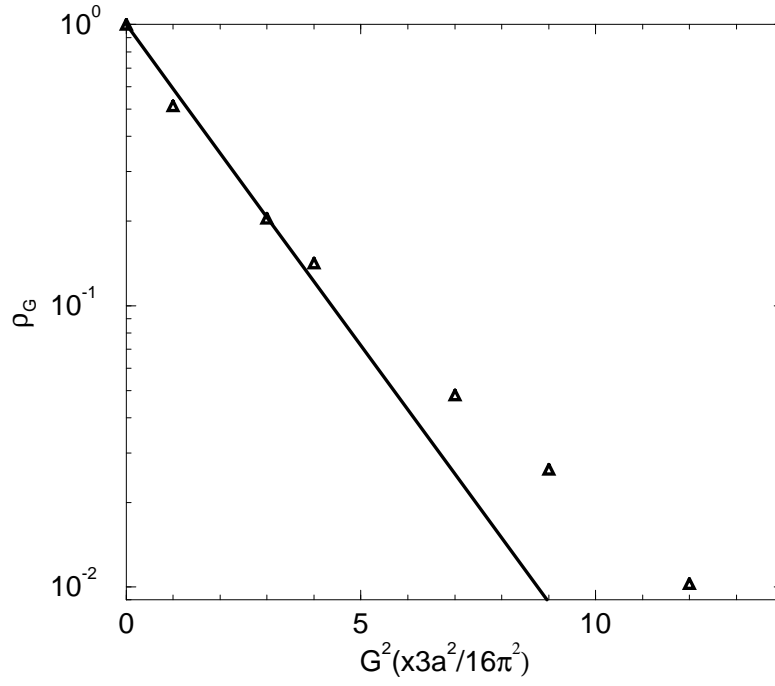


FIG. 6. Fourier components $\rho_{\mathbf{G}}$ of the periodic density field at the freezing temperature, as calculated in the density functional theory (triangles), plotted versus $|\mathbf{G}|^2$ on a semi-logarithmic scale. The solid line corresponds to a Gaussian form for ρ_G (see text) which has the same Debye-Waller factor as that obtained in the density functional theory at the freezing transition.

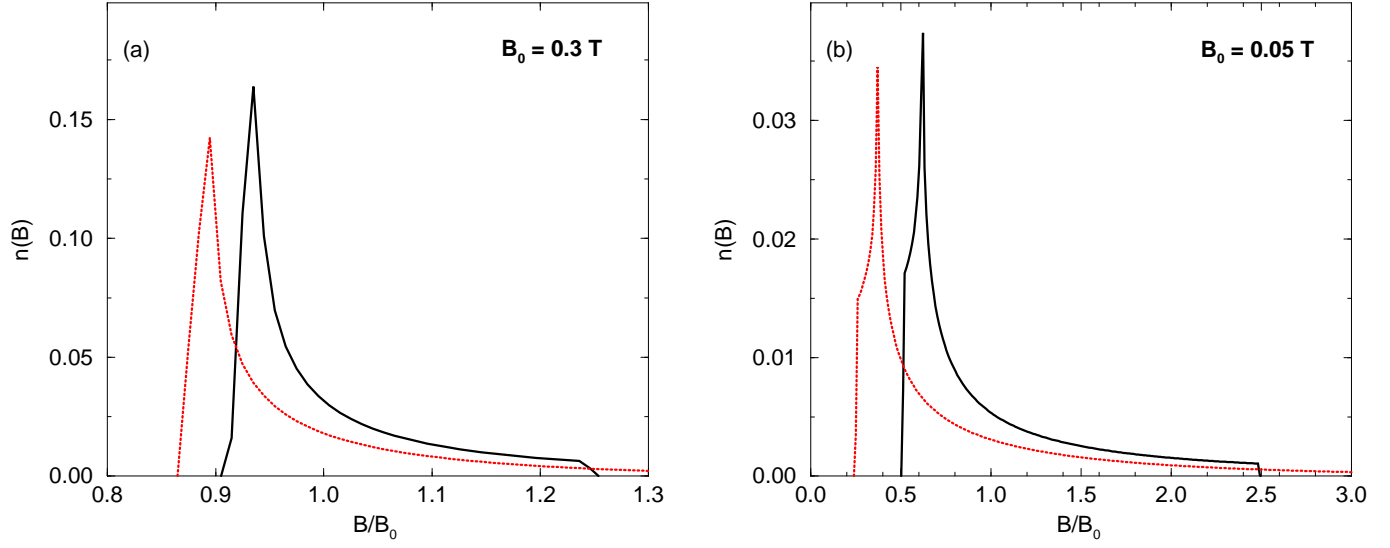


FIG. 7. Magnetic field distribution function $n(B)$ in the crystalline phase at the freezing temperature for (a) $B_0 = 0.3$ T and (b) $B_0 = 0.05$ T. The thermally broadened time-averaged density distribution in the crystalline state is obtained using the results of the density functional theory. The distribution $n(B)$ for a slightly broadened Abrikosov flux-lattice (dashed lines) is also shown for comparison. Note that the distribution given by the density functional calculation is considerably narrower and more symmetric.

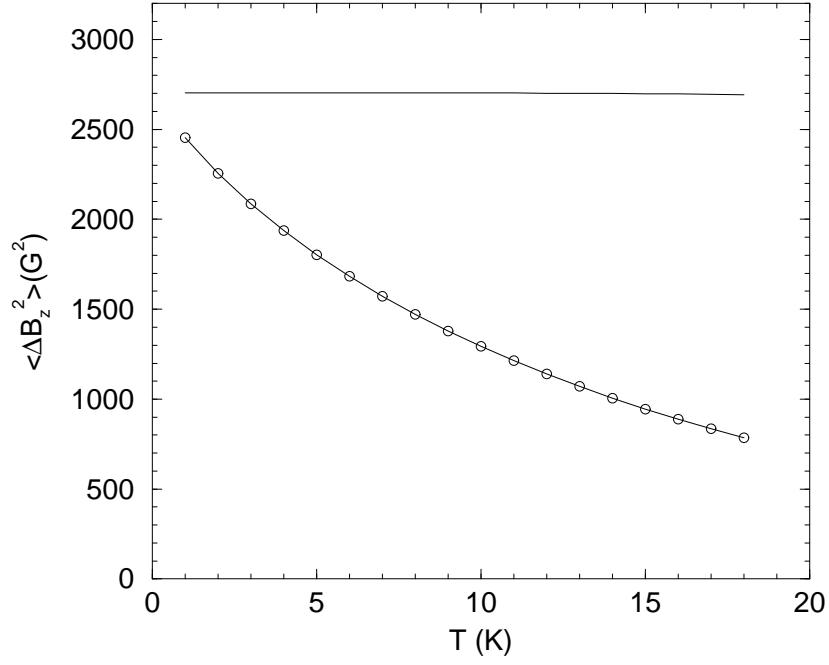


FIG. 8. The second moment $[\Delta B^2]$ of the magnetic field distribution $n(B)$ versus temperature T for $B_0 = 0.3$ T, obtained using the results of density functional theory for the Fourier components of the density field and a Debye-Waller approximation for the low-temperature regime. For comparison, the results for a perfect Abrikosov lattice are also shown (solid line). Corrections due to a finite core size (see text) are included. Note the curvature of the moment as a function of T , which is opposite to that obtained for a perfect Abrikosov lattice assuming a two-fluid form for the temperature dependence of λ .

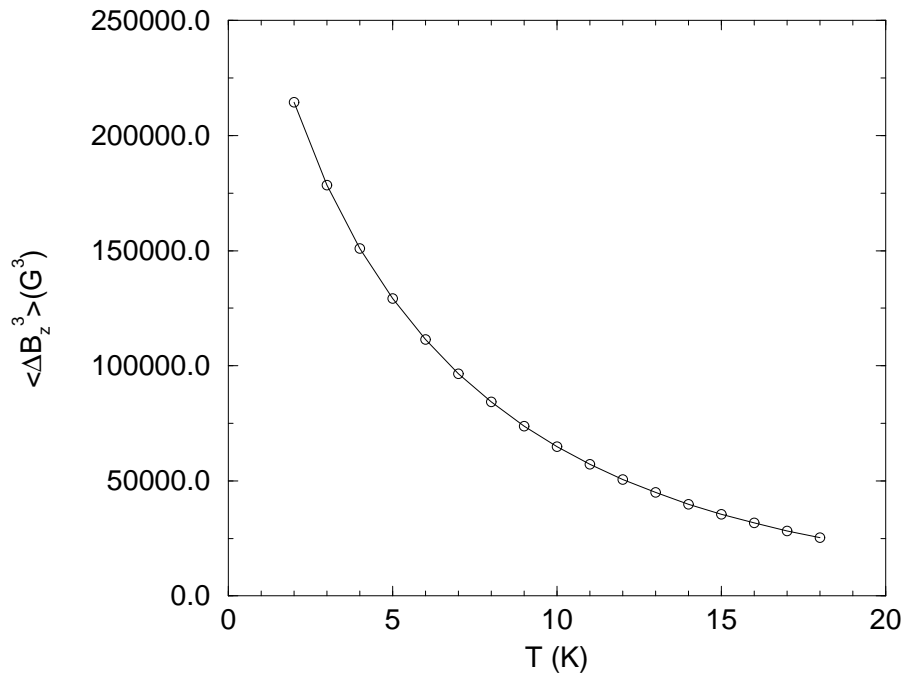


FIG. 9. The third moment $[\Delta B^3]$ of the magnetic field distribution $n(B)$ versus temperature T for $B_0 = 0.3$ T obtained using the results of density functional theory for the Fourier components of the density field at the freezing transition and a Debye-Waller approximation for the low-temperature regime. Corrections due to a finite core size (see text) are included.